LBL-14590

Solar & Wind Technology Vol. 4, No. 3, pp. 347-379, 1987
Printed in Great Britain.

0741-983X/87 $3.00 + .00
Pergamon Journals Ltd.

ADVANCED OPTICAL MATERIALS FOR ENERGY EFFICIENCY AND SOLAR CONVERSION

CARL M. LAMPERT
Applied Science Division and Materials and Chemical Sciences Division, Lawrence Berkeley Laboratory, (MS 62-203) University of California, Berkeley, CA 94720, U.S.A.

(*Received* 10 *July* 1986; *accepted* 20 *August* 1986)

Abstract—Materials science properties of optical materials and coatings are discussed for a broad range of solar conversion, architectural glazings and greenhouse energy efficient uses. Transparent low emittance coatings for glazings are discussed for radiative heat transfer reduction. Both interference multilayer and doped semiconductor low emittance coatings are covered. The use of Drude theory to model coatings is discussed. Discussion of various types of selective absorbers include interference multilayer, composite tandem absorbers and selective paints. Effective medium theories are used to describe composite absorbers. The basic properties of radiative cooling materials and antireflection coatings are detailed. Also, the properties of reflector materials on glass and plastics are covered. Application of fluorescent concentrators, spectral splitting and cold mirror films are outlined. Research on transparent aerogel insulation and optical switching films for windows are introduced.

INTRODUCTION

Optical materials and coatings play an important role in determining the efficiency of solar conversion processes. At present the best known coatings are heat mirrors, selective absorbers, and reflector materials. There are, however, many less known coatings and materials, some of which are under current research and development. Since they are of significant consequence to solar conversion and energy conservation, they will be included in this work. These films and materials are known as antireflective coatings or treatments, fluorescent concentrator materials, holographic films, cold mirrors, radiative cooling surfaces, optical switching films and transparent insulation materials. The use of such films and materials improves the efficiency and stimulates innovation in passive and active solar energy conversion, photovoltaics, energy-efficient windows and many hybrid designs. The present study is intended to instruct readers on the properties of solar energy materials and their function, as well as advantages and limitations. It is also intended to expand the horizons of solar invention by considering new materials, techniques and concepts that can manipulate solar energy into the forms of heat, light and electrical power. The material stability requirements for effectively collecting and transmitting solar energy are extremely demanding. This combined with the need for inexpensive production methods creates a very broad area for innovative scientific research. The solutions to materials science and design problems are the responsibilities of a number of scientists, engineers and educators working in many countries and in numerous fields. It is their strong commitment to solar energy that will further advance this energy source.

BASIC THEORY

The optical engineering properties that are of primary interest for most solar materials are transmittance (T), reflectance (R), absorptance (A) and emittance (E). These properties characterize how a particular coating or a material interacts with incident energy. Furthermore, these qualities can be related to intrinsic material properties such as the index of refraction (n) and the extinction coefficient (k). Also all these properties have a spatial, wavelength or temperature dependence. Formally, the spectral transmittance (T_w) is the ratio of incident radiation transmitted through a medium at wavelength w, to that of the total incident radiation at w.

The spectral reflectance (R_w) is the ratio of incident radiation reflected from the medium at w to the total incident radiation at w. The spectral absorptance (A_w) is the ratio of incident radiation absorbed in the medium at w to the total incident radiation at w. A relationship between these quantities allows for

conservation of energy:

$$A_w + R_w + T_w = 1.$$

The thermal emittance $[E(T)]$ is defined as the ratio of emitted radiation from a surface at Temperature T to the corresponding blackbody radiation at T. The spectral quantities of A_w and E_w are equivalent, provided that the measurements are taken at the same temperature and under the same conditions:

$$A_w(T) = E_w(T).$$

In practice these properties are best represented as integrated values. Total solar absorptance can be defined as:

$$A_s = \frac{\int_{0.3}^{2.5} A_w I_w \, dw}{\int_{0.3}^{2.5} I_w \, dw},$$

where w is in microns and (I_w) is defined as the solar irradiance at w at some air mass. For a selective absorber, $T_w = 0$ and A_w can be defined from reflectance measurements as:

$$A_w = 1 - R_w.$$

Similar integrations can be made for R_s and T_s. The total thermal emittance $E_T(T)$ can be defined as:

$$E_T(T) = \frac{\int_{1}^{100} E_w(T) B_w(T) \, dw}{\int_{1}^{100} E_w(T) \, dw},$$

where w is in microns and $B_w(T)$ is the radiation intensity (given by the Planck function) for a blackbody at temperature T, the same temperature of the object being measured. For heat mirrors and other transparent coatings the visible transmittance is important. Although much reported data are cited as visible transmittance, these are usually only averaged data and not integrated. T_v is defined as follows:

$$T_v = \frac{\int_{0.39}^{0.77} T_w P_w \, dw}{\int_{0.39}^{0.77} P_w \, dw},$$

where w is in microns.

In this case the distribution function is the photopic or specular eye response distribution (P_w). This distribution is Gaussian in nature and peaks in the green wavelengths (0.55 μm).

TRANSPARENT HEAT MIRRORS

Heat transparent mirror or low emittance coatings play a significant role in solar thermal conversion [1] transparent insulation for architectural windows [2] and photovoltaic conversion [3]. In this work a heat mirror is defined as a coating that is predominately transparent over the visible wavelengths (0.3–0.77 μm) and reflective in the infrared wavelengths (2.0–100 μm). Over the near infrared (0.77–2.0 μm) the coating may exhibit combined properties depending upon design or application requirements. Figure 1 shows an example of an idealized heat mirror response superimposed on solar and blackbody radiation spectra. Heat mirrors for windows derive their usefulness from their low emittance (or high reflectance) in the infrared. The lower the emittance, the less the magnitude of radiative transfer by the window. The emittance of glass is $E_T = 0.84$; many plastics also have high emittance values. Two scenarios can be invoked to demonstrate the usefulness of single glazed heat mirrors in buildings [2]. The first scenario, depicted in Fig. 2, represents winter heating where solar gain is important to reduce the heating load in a building. The optimum heat mirror for this function would transmit both solar visible and near infrared to about 2–3 μm, the cut off wavelength for glass. The thermal infrared would be reflected back into the building. In this process the majority of the solar energy could be utilized for passive solar gain and daylighting.

A second scenario can be treated as a cooling-load-reducing heat mirror, where all infrared energy is reflected to reduce air conditioning loads. This type of heat mirror is depicted in Fig. 3. The coating allows only transmission of visible energy through the window, with the remainder of the wavelengths

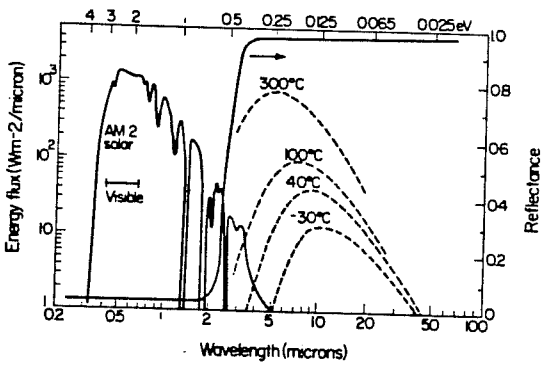

Fig. 1. Solar spectrum (air mass 2) with four blackbody spectra (−30–300°C). Superimposed is the idealized reflectance of a heat mirror coating

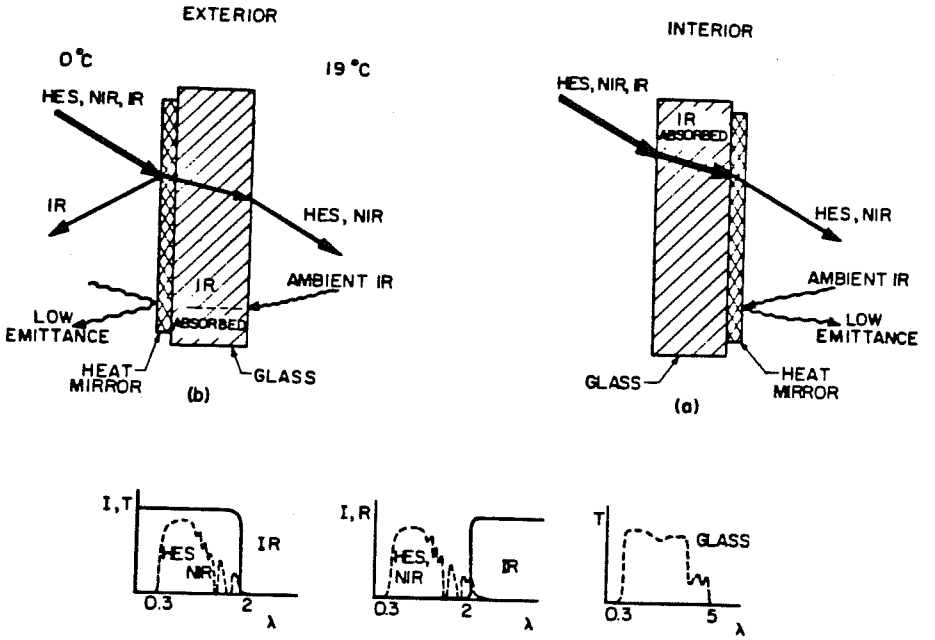

Fig. 2. Schematic of heating-load heat mirror properties. Lower drawings depict optical properties of coating and substrate.

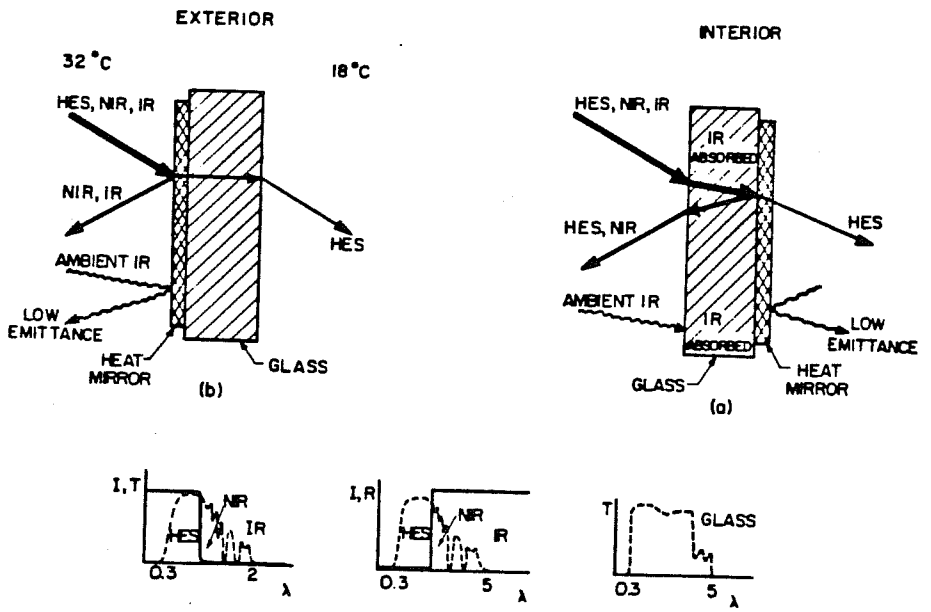

Fig. 3. Schematic of cooling-load heat mirror properties. The exterior placement is subject to convection losses that can lessen the benefit.

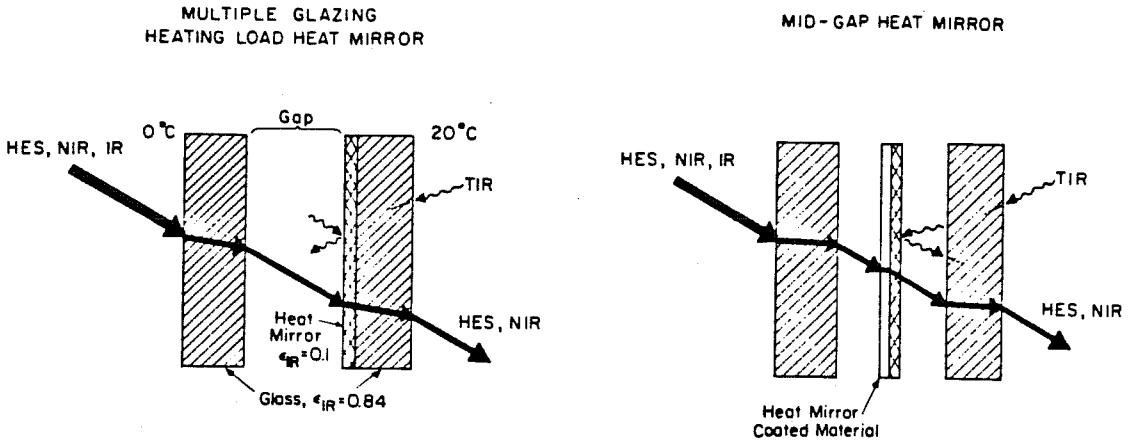

Fig. 4. Double and triple glazed windows incorporating heat mirrors.

reflected. A heat mirror alters only the radiative character of a window; the effects of convective and conductive heat losses must be taken into account, too. Window orientation, climate and building type are important factors in choosing the exact combination of optical properties the heat mirror is to have. A film with adjustable properties might be the best solution.

Examples of multiple glazed heat mirrors are shown in Fig. 4. Here both a double and triple glazed window are shown. One design depicts a heat mirror coating on plastic. Deposition of heat mirrors on glass and plastic substrates are of significant importance. One fits well into conventional glass coating processes and the other is a refined extension of the metallizing process for plastics. By use of a computer model [4], thermal conductance (U) values have been derived for various types of glazings. These data are shown in Fig. 5. A nonglass insulated wall has thermal conductance values of $U = 0.3$ W/m^{2}K (R-19) to $U = 0.6$ W/m^{2}K (R-11).

A heating-load heat mirror could also be used for solar thermal collectors as an alternative to selective absorbers. But, in this case, the heat mirror could be used with a nonselective absorber. One modification of this heat mirror is to shorten the transition or cut off reflectance wavelength, which would be more suitable for higher operating temperatures of solar collectors. The results of using a heat mirror coating on a double glazed flat plate plate collector are shown in Fig. 6. Also shown for comparison is the effect of using a selective absorber and antireflective coatings [5]. These coatings will be discussed in subsequent sections. Transparent conductors as heat mirrors can be physically deposited (PVD) on glass and plastic by

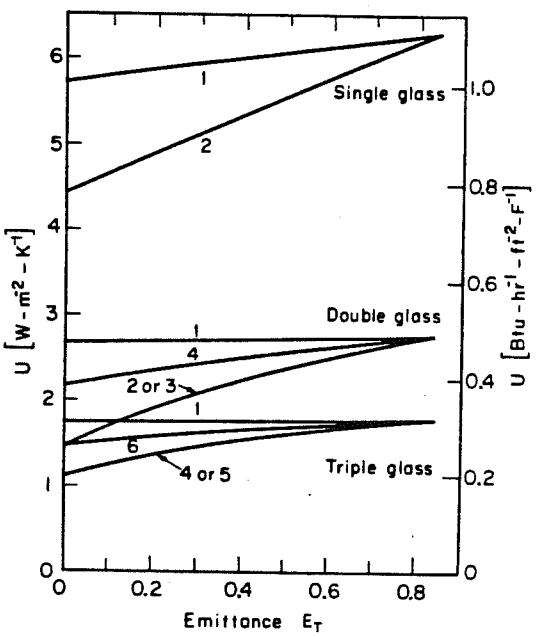

Fig. 5. Computer-modeled thermal conductance (U) for various window designs [4] using ASHRAE standard winter conditions ($T_{out} = -18$ C, wind speed = 24 km hr). The effect of lowering the emittance of a single surface by the addition of a heat mirror coating is shown. The surfaces on which the coating appears are given as consecutive numbers, starting from the outside surface, labeled 1. Airgap is 1.27 cm.

vacuum evaporative and sputtering techniques. Methods, including chemical vapor deposition (CVD) and polycondensation of organometallics, have been limited mostly to glass. The thermal and chemical stability of the substrate are significant in deter-

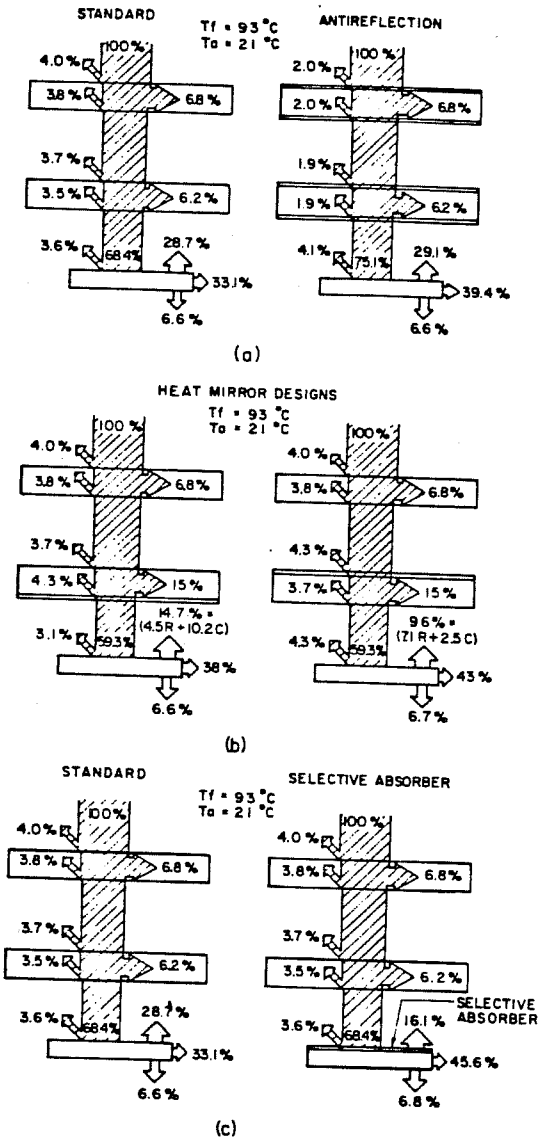

Fig. 6. The effect of various coatings on collector efficiency [5] for a flat plate collection operating at 93 C under an ambient temperature of 21 C. The notation *R* stands for reflection losses, and *C* stands for convection losses.

mination of the proper technique and conditions. With CVD the secondary and competing reactions must be suppressed by control over reaction kinetics and knowledge of system thermodynamics. Also, thermal durability and property stability of substrate and film is significant for long-life designs. Heat mirror films can be classified into two categories: multilayer dielectric/metal-based films such as Al_2O_3/Ag, ZnS/Cu/ZnS and TiO_2/Ag/TiO_2 and single-layer semiconductors (highly doped) such as In_2O_3:Sn and SnO_2:F. There is considerable growing interest in both multilayer and semiconductor heat mirrors in Europe, North America, USSR, East Germany and Japan. Further information on heat mirrors is contained in a number of excellent works [2, 3].

Multilayer heat mirror films

Metal films less than approximately 100 Å thick exhibit partial visible and solar transparency. Dielectric overlayers serve to both protect and partly antireflect the metal film in the visible region, thereby increasing transmission. Generally though, further protection is required for the metal/dielectric film as it is quite thin and vulnerable to corrosion and abrasion. The design of the appropriate dielectric type and thickness is detailed elsewhere [6]. The dielectric film, when used to overcoat a metal, must exhibit high infrared transmittance in order to preserve the infrared reflectance of the metal. Example systems [2] are SiO_2/M, polymer/M, Al_2O_3/M, Bi_2O_3/M, Bi_2O_3/M/Bi_2O_3, ZnO/M/ZnO, TiO_2/M/TiO_2 and ZnS/M/ZnS, where M is a metal of Ag, Al, Au, Cu, Cr, Ni and Ti. Additional designs include X/M and X/M/X where X is an appropriate semiconductor or polymer. Infrared transparent polymers of polyethylene, polyvinylidene chloride, polyacrylonitrile, polypropylene and polyvinyl fluoride might be used for this application. Multilayer films have an advantage over the doped semiconductors of broad wavelength tunability. Some selected multilayer films on glass and plastic substrates [7–10] are shown in Figs 7 and 8. Detailed property data on these films are shown in Table 1. Extensive data on D/M/D coatings are covered elsewhere [2]. Durability improvement of multilayer films still remains an important research area for the materials scientist. A recent review details the properties of various types of commercial heat mirror coatings, including both multilayer and single layer types [11].

Doped semiconductor films

Certain doped semiconductors can exhibit high infrared reflectance due to the proper combination of high mobility (> 10 cm^2/V sec) carrier concentration (10^{20}–10^{23} cm^{-3}) effective mass and lattice relaxation frequency. Materials science details are outlined elsewhere [13]. The best known transparent semiconductors are SnO_2:F, SnO_2:Sb, In_2O_3:Sn, and Cd_2SnO_4. Characteristic spectral transmission and reflectance is shown in Fig. 9 for research-grade films on glass [14–16]. The transmission of these films can

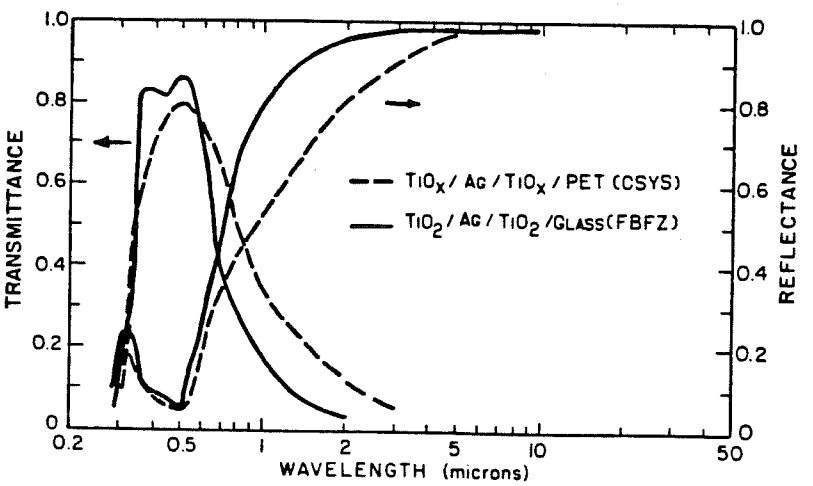

Fig. 7. TiO_2/Ag/TiO_2 coating on polyethylene terephthalate [7] (PET) and glass [8].

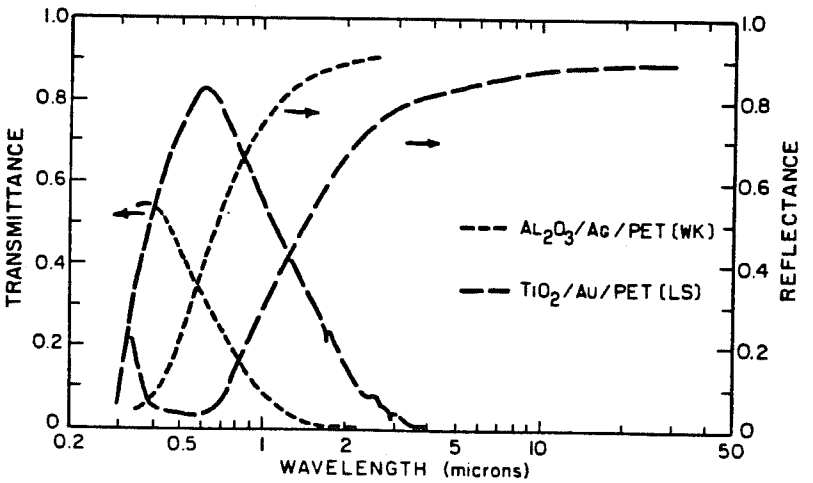

Fig. 8. Dielectric/metal coatings on PET [9, 10].

Table 1. Multilayer heat mirror films

Material	Al_2O_3/Ag	TiO_2/Au/PET	TiO_2/Ag/TiO_2	TiO_x/Ag/TiO_x	ZnS/Ag/ZnS
Deposition tech.	Ion Beam Sputter	e-Beam Evap. and Chemical Dep.	RF Sputter	Chemical Dep. and Vac. Evap.	Vac. Evap.
Sheet Resist. (ohm/sq)	—	10	—	—	10
Thickness (angstroms)	—	—	180/180/180	270/150/270	520/100/770
T_{vis}(ave) or T_s	0.47, 5 μm	0.80	0.84	~0.75	0.68
R_{ir} or (E_{ir})	0.93, 2.5 μm	0.87	0.99, 10 μm	0.98, 5 μm	(0.06)
Reference	[9]	[10]	[8]	[7]	[12]

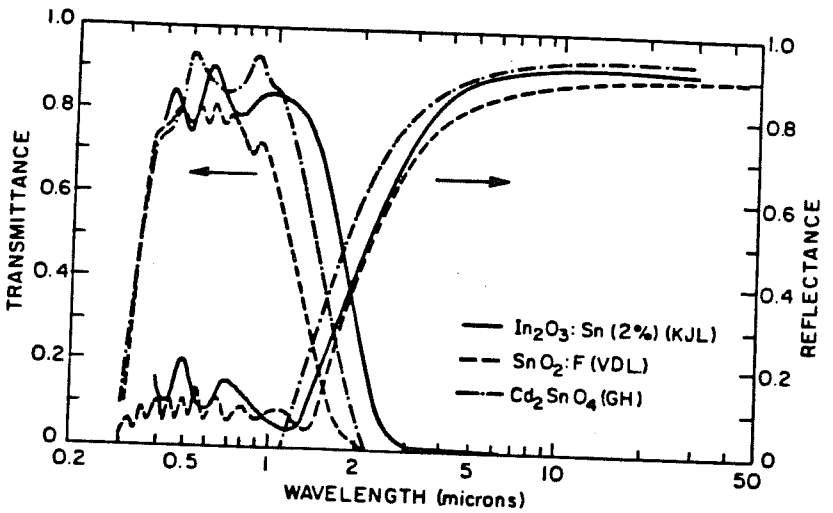

Fig. 9. Spectral normal transmittance and reflectance of heat mirror research-grade film on glass based on In_2O_3: Sn, SnO_2: F_3 and Cd_2SnO_4 [14–16].

be increased by etching microgrids in the coatings [17]. Obtaining a reproducible high-quality commercial coating is considerably more difficult than making research-grade films. Present techniques need to be improved to deposit these coatings on polymeric substrates [18, 19]. Specific examples of these films are shown in Fig. 10. Table 2 lists the physical properties of selected doped semiconductor films. Detailed information on depositon processes are given elsewhere [2, 13, 20–23]. There are other promising heat mirror materials. They include some of the rare earth oxides, borides, transition metal nitrides, carbides and selected ternary systems. Although little knowledge has been obtained optically about these materials, they are known to exhibit Drude-like electrical conduction. Also, graded index and surface textured heat mirror coatings remain to be developed. They show promise of improved solar transmission characteristics.

Theory of Drude-like coatings

Both highly doped semiconductors and thin metal films are linked by the conductive metal-like prop-

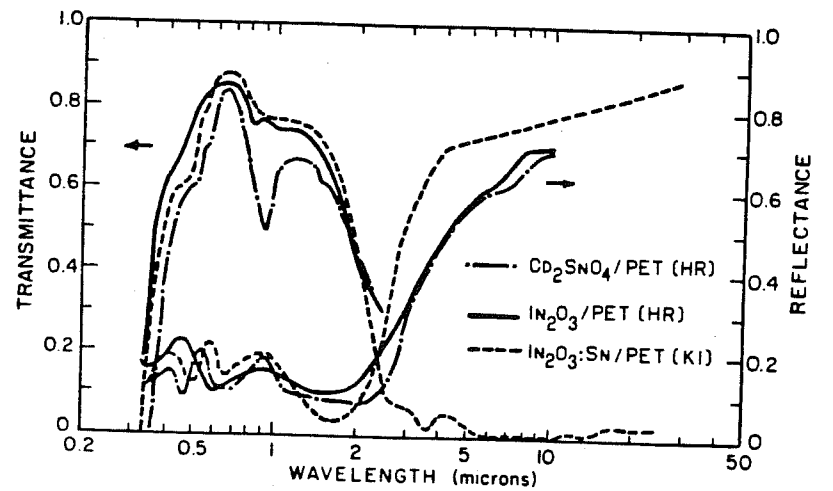

Fig. 10. Spectral normal transmittance and reflectance of single-layer heat mirror coatings deposited on polyethylene terephthalate [18–20].

Table 2. Selected heat mirror films

Material	SnO_2:F	Cd_2SnO_4	In_2O_3:Sn	In_2O_3:Sn
Deposition tech.	Spray Hydro. 500–570 C	RF Sputt. Anneal 420 C	Spray Hydro.	RF Sputt. etched microgrid
Sheet Resist. (ohm/sq)	4	26–43	15–20	3
Thickness (microns)	1.0	< 0.3	—	0.35
Mobility (cm^2/V-sec)	37	—	—	—
Carrier Density ($cm^{-3} \times 10^{20}$)	4.4	—	15	—
T_{vis}(ave) or (T_s)	(0.75)	(0.86)	~ 0.9	(0.90, AM2)
R_{ir} or (E_{ir})	(0.15)	(0.12, 77 C)	0.85	0.83, 10 μm
Reference	[16]	[15]	[14]	[17]

Material	Cd_2SnO_4/PET	In_2O_3/PET	In_2O_3:Sn/PET
Deposition tech.	React. DC Sputt. and RF BIAS	React. DC Sputt. and RF BIAS	React. RF Sputt.
Sheet Resist. (ohm/sq)	24	30	< 30
Thickness (microns)	0.28	0.34	0.5
Mobility (cm^2/V-sec)	30	29	—
Carrier Density ($cm^{-3} \times 10^{20}$)	3.4	2.1	—
T_{vis}(ave)	~ 0.65	~ 0.78	0.8
R_{ir} or (E_{ir})	0.7, 10 μm	0.7, 10 μm	0.8, 10 μm
Reference	[18]	[18]	[19]

erties described by classical Drude theory [24]. In this theory, a well-defined plasma edge characterizes the material. It occurs due to excitation of free carriers by incident electromagnetic radiation. Since the charge carriers are actually moving in a potential field of the crystal, an effective mass (m^*) must be used. The effective mass is defined as:

$$m^* = m_r m_e,$$

where m_e is the rest mass and m_r is the relative mass of the charge carriers in the field. The complex dielectric constant is related to the optical constants by:

$$e = e_1 + ie_2 = (n - ik)^2,$$

$$\text{where} \quad e_1 = n^2 - k^2 \quad \text{and} \quad e_2 = -2nk.$$

For a Drude-like reflector, the dielectric constant can be expressed in terms of (V/v_p) and (Y/v_p) as follows:

$$e_1 = e_b\left[1 - \left(1 + \left(\frac{Y}{v_p}\right)^2\right)\Big/\left(\left(\frac{V}{v_p}\right)^2 + \left(\frac{Y}{v_p}\right)^2\right)\right],$$

$$e_2 = e_b\left[\frac{Y}{v_p}\left(1 + \left(\frac{Y}{v_p}\right)^2\right)\Big/\frac{V}{v_p}\left(\left(\frac{V}{v_p}\right)^2 + \left(\frac{Y}{v_p}\right)^2\right)\right].$$

where e_b is the dielectric constant associated with bound carriers (at very high frequency) and Y is the relaxation frequency, $Y = e/um_e$. u is the carrier mobility, and e is the electron charge. The damped plasma frequency (v_p) is derived as:

$$v_p = (Ne^2/e_b e_o m^*)^{1/2} - Y^2,$$

where N is the carrier density and e_o is the dielectric constant of air. From this theory, n and k can be extracted in terms of frequency (W). Reflectance in air (normal-specular) can be derived by:

$$R = ((n-1)^2 + k^2)/((n+1)^2 + k^2).$$

The theoretical reflectance for a highly doped transparent conductor is shown in Fig. 1. The Drude-modeled reflectance agrees well with that obtained by experimental doped semiconductor films. One should note that in the Drude equation as $V \gg v_p > Y$, n becomes constant and $k \to 0$, indicating that the material is transparent at short wavelengths and for $V \ll Y < v_p$, $n = k$ are about equal and large in magnitude, indicating a high reflectance.

SOLAR SELECTIVE ABSORBERS

Absorbers for collectors have been one of the most active materials science research fields over the last few years. There are two categories of absorbers, selective and nonselective. The selective absorber has optical properties that vary greatly from one spectral region to another. The selective absorber or selective surface efficiently captures solar energy in the high-intensity visible and the near-infrared spectral regions while exhibiting poor infrared radiating properties. This characteristic is depicted in Fig. 11. In contrast a nonselective absorber, such as ordinary black paint, has a flat spectral response and loses much of its absorbed energy by reradiation. The optimum characteristics of a solar absorber are high solar absorptance and a minimum emittance (or maximum reflectance) in the infrared wavelengths. The exact transition wavelength is determined by application, solar concentration and operating temperatures. Examples of concentrating collector designs are shown in Fig. 12. Solar selectivity can be obtained by a variety of methods. These techniques consist of intrinsic solar selective materials, optical trapping surfaces, semiconductor/reflector tandems, composite coatings, multilayer thin films and quantum size effects. Significant reviews have been written about solar absorbers, giving insight and detail beyond the scope of this work [1, 25–29]. A selected group of solar selective absorbers is outlined in Table 3 after Herzenberg and Silberglitt [26].

Intrinsic absorbers

No known natural compound or material exhibits ideal solar selectivity. However, there are some materials that show wavelength selectivity to some degree. Possibly, synthetic materials could be fabricated once enough knowledge is obtained to design and predict fairly complex electronic structures and their relationships to the necessary optical properties. Both transition metals and heavily doped semiconductors exhibit at least one desirable absorber characteristic. Unfortunately, metals exhibit a plasma edge too early in the solar spectrum to be good absorbers. Semiconductors tend to be good absorbers but exhibit transmission in the infrared. These differences have resulted in the use of tandem absorbers. Materials such as Cu_2S, HfC, ZrB_2 Mo–MoO_3, Na_xWo_3, Eu_2O_3, V_2O_5, ReO_3, and LaB_6 (as shown in Fig. 13) have reasonably intrinsic selective reflectance. Here, too, the dominant transition takes place too early in the solar spectrum for a good absorber. Also, the absorptance and transmittance properties are not well characterized. Lanthanum hexaboride may be a good heat mirror, since it has fair visible transmittance.

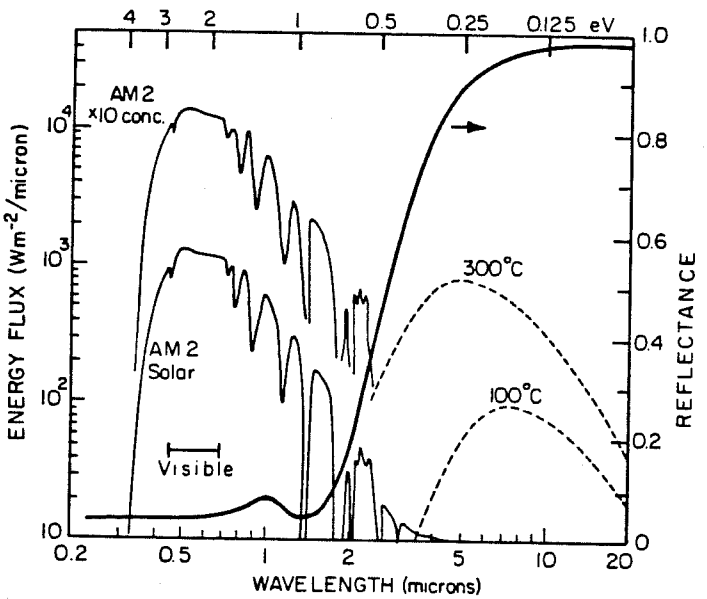

Fig. 11. Wavelength relationship between a characteristic black chrome solar selective surface in terms of reflectance, to that of solar energy and blackbody spectra. Both concentrated ($\times 10$) and regular solar spectra for air mass 2 are given.

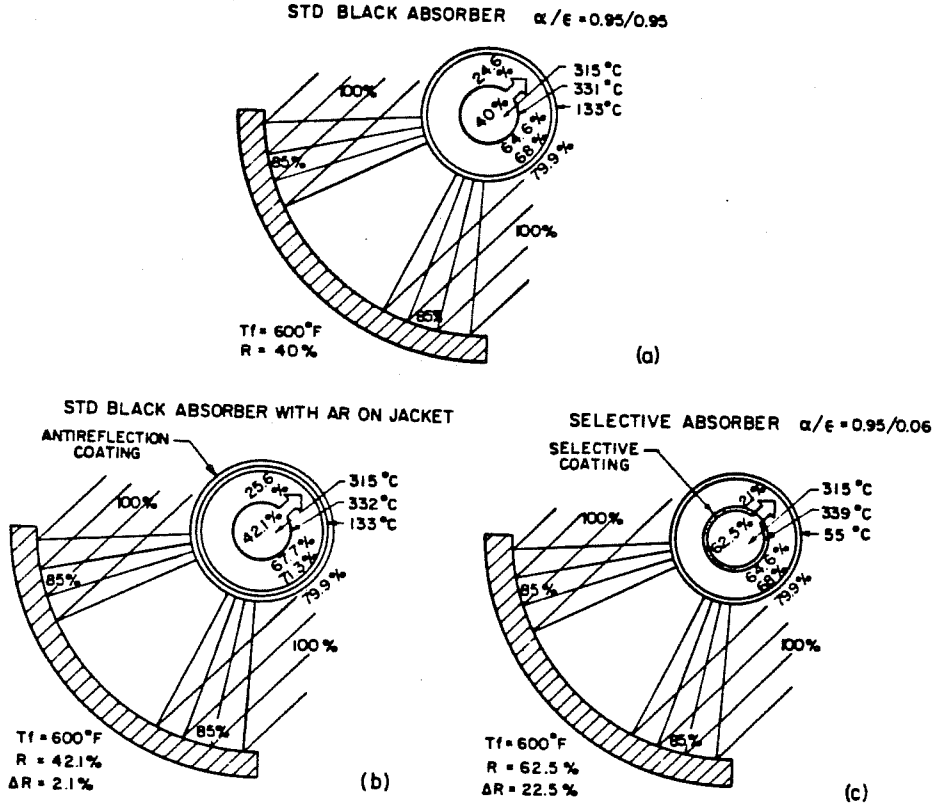

Fig. 12. Fixed conditions for a parabolic concentrating evacuated collector [80]. The collector is operating at 315°C with ambient temperature of 21°C. Notation: R = net collection efficiency, ΔR = change in collecting efficiency over a standard black absorber and T_f = fluid temperature.

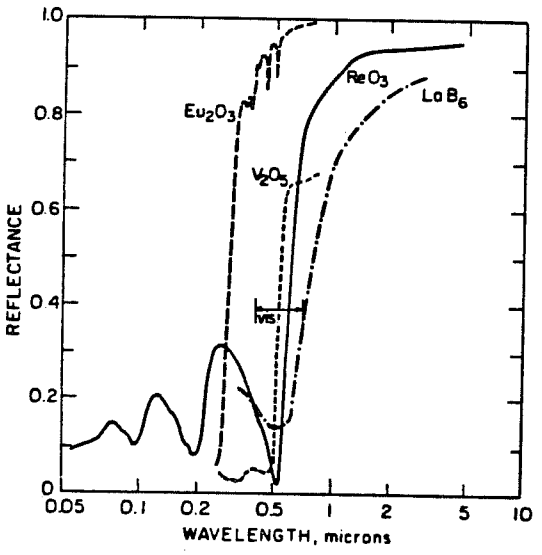

Fig. 13. Spectral reflectance of various oxides showing intrinsic wavelength sensitivity [13].

Optical trapping surfaces

It is possible to roughen surfaces so they will enhance absorption geometrically in one wavelength region but appear smooth in another. This technique is possible since the high-energy solar spectrum is distributed far enough in wavelength away from the thermal infrared spectra. Materials can be grown as dendrites, rough crystallites, or roughened surfaces to form optical trapping surfaces as in Fig. 14. These dendritic materials do not require a high intrinsic absorption as they rely upon multiple reflection and partial absorption to give a large effective absorption. Materials such as $NiAl_x$, W, Mo, Ni, Cu, Fe, Co, Mn, Sb, and stainless steel have been grown as dendrites or textured by sputter etching [1, 31, 56]. Texturing of surfaces is also an excellent method to antireflect other types of absorbers. This has been done with great success with the Mo–Al_2O_3 composite absorber [54].

Semiconductor/metal tandems

Semiconductor coated metals provide complementary functions as a spectrally selective surface.

Table 3. Properties of selective absorbers [26]

Absorber*	Type	Deposition technique	Maturity†	A_s	E(°C)	Stability‡ °C	Ref.
Copper	Textured	Sputter etch	1	0.9–0.95	0.08–0.11	300(air)	31
SS	Textured	Sputter etch	1	0.9–0.96	0.22–0.26	350(air)	31
Ni	Textured	Sputter etch	1	0.9–0.95	0.08–0.11 (27)	250(air)	31
ZrB_2/Si_3N_4	AR Intrinsic	CVD	1	0.93	0.08–0.09 (102)	500(air)	30
$Cr–Cr_2O_3$ (black chrome)	Graded Composite	Electroplating	5	0.92–0.97	0.04–0.06 (100)	400(air)	32–34
$Cr–Mo–Cr_2O_3$	Graded Composite	Co-electroplating	1	0.96–0.97		400(air)	35
$Ni–Al_2O_3/Al_2O_3$	Graded Composite	Anodic Oxidation	5	0.92–0.97	0.1–0.26 (65)	300(air)	36
Zn–ZnO	Graded Composite	Anodic Oxidation	1	0.98	0.18(100)	< 30(air)	37
$Cu_2O–CuO–Cu$	Composite/ Tandem	Anodic Oxidation	1	0.95	0.34(100)	130(air)	38
$NiO–Ni–Cr/NiCrO_x$	Graded Composite	Chemical Conversion	5	0.97–0.99	0.07–0.1 (100)	250(air)	39, 44
SS–C	Graded Composite	Reactive Magnetron Sputtering	5	0.94	0.03–0.1 (100)	300(vacuum) 200(air)	40
SS–C (on rough sputtered copper)	Textured Composite	Reactive Mag. Sput.	3	0.9	0.04(67)	450(vacuum)	41
$SS–SSO_x/SSO_x$	AR Composite	Reactive Mag. Sput.	1	0.89–0.93	0.08(20)	150(air)	42
$Cr–Al_2O_3$	Graded Composite	Dual Source Mag. Sput.	1	0.92	0.09(20)		42
$Mo–MoO_2/Si_3N_4$	Composite/ Intrinsic	CVD	1	0.91	0.11(500)	500(vacuum) 300(air)	43
Tellurium	Textured Tandem	Angled Vapor Deposition	1	0.92	0.03		47
$a–Si/Si_3N_4$	AR Tandem	CVD	1	0.75	0.08(500)	500(air)	48
Cu_2S	Tandem	Chemical Spray Dep	1	0.89	0.25(100)	130(air)	49
CoO	Textured Graded Tandem	Electropl. + Heat Oxidation	1	0.98	0.2(100)	425(air)	50
$CoO–FeO_3–Co_3O_4$	Textured Tandem	Electropl. + Heat Oxidation	1	0.9	0.07(100)	300(air)	51
$Ge–CaF_2$	Composite	Sputtering	1	0.65–0.72	0.01–0.1 (100)		52
Ge	Textured Tandem	RF Sputt. H_2O_2 etching	1	0.98–0.99	0.58		53
AMA (M = Cr)	3-layer	Re. Mag. Sput.	3	0.95	0.12(20)	300(air)	45
AMA (M = Ni)	3-layer	Re. Mag. Sput.	3	0.91	0.08(20)	300(air)	45
AMA (M = Ta)	3-layer	Re. Mag. Sput.	3	0.89	0.12(20)	300(air)	45
Proprietary	3-layer	Elect. Beam. Evap.	3	0.92–0.96	0.05–0.08	250(air)	26
$Al_2O_3/Pt–Al_2O_3/Al_2O_3$	3-layer Composite	RF Mag. Sput.	3	0.91–0.93	0.08–0.1 (20)	> 600(air)	45
$Al_2O_3/Mo–Al_2O_3MO$	Composite	Co-evap.	1	0.99	0.2(500) 0.08(200)	750(vac)	54
ZrC_x/Zr	Tandem	RF Sput.	3	0.93	0.25	625(vac)	55
$Cr–CrO_x$	Composite on Al foil	Re. Evap.	3	0.9	0.05	175	55
Ni–C	Composite	Sputtering	1	0.8	0.028–0.035 (150)		46
NiN_x	Tandem	Sputtering	1	0.84	0.039(150)		46

* Absorber layers are separated by a "/". Constituents of composite layers are separated by a "–".
† Maturity of absorber coatings: 5 commercial, 3 development, 1 research.
‡ Temperature stability for most absorbers is not well known.
Abbreviations: AR-antireflected; CVD-chemical vapor deposition; Mag. Sput.-magnetron sputtering; Electropl.-Electroplating; RF-Radio Frequency; Re.-Reactive; Elect.-Electron; Evap.-Evaporation.

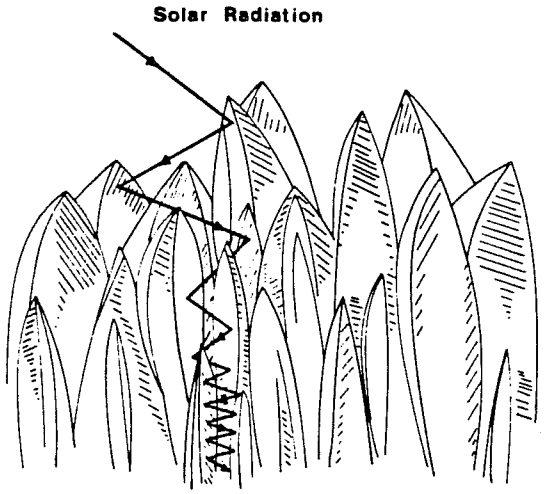

Fig. 14. Dendritic selective surface.

The semiconductor provides high absorptance in the high-energy solar region and becomes transparent beyond its absorption edge in the infrared. In the infrared the underlying metal layer gives the tandem or metallic reflectance as low emittance. A simple tandem is an oxidized metal. Usually the natural thickness of oxide is not optimum or is not stable in operation. Many chemical conversion processes are used to oxidize metals [1]. Metals like stainless steel, copper and titanium have been oxidized. Other tandems can be made with deposits of oxides on a variety of metals. Examples are shown in Fig. 15. High temperature absorbers can also be designed, such as the Si/Ag absorber which is stable to 500 C [27]. Tandem absorbers can be made by simple chemical conversion, electrochemical deposition, chemical vapor deposition (CVD) and physical vapor deposition processes (PVD) (sputtering and evaporation). Composite coatings can also be used as the absorber portion of tandem absorbers.

Metal-dielectric composite and graded coatings

Composite coatings consist of two or more components graded and interdispersed in a film. These components are usually phase separated. Reflective scattering can take place purely by the geometry of imbedded surface particles. Resonant scattering is dependent upon particle size, shape and the effective index of refraction with respect to the surrounding media. Both Mie and Maxwell–Garnett theories describe the role of subwavelength particles as resonant scatters [60]. An example of a complex composite material is the well-known black chrome absorber depicted in Fig. 16. This coating consists of a predominantly oxide region that grades to a Cr_2O_3–Cr region that is responsible for solar absorption. Infrared properties are derived from a deeper metallic chromium region coupled with a metallic substrate [61–64]. Further research on black chrome has been reviewed elsewhere [26]. Other types of composites range from Ni–Al_2O_3, Zn–ZnO, Cr–Cr_2O_3, Pt–Al_2O_3, Mo–Al_2O_3, and metal carbides. Many of their properties are detailed in Table 3. Composite coatings of black chrome, $NiCrO_x$, and Cr–CrO_x have been deposited on thin metal films for stick-on applications

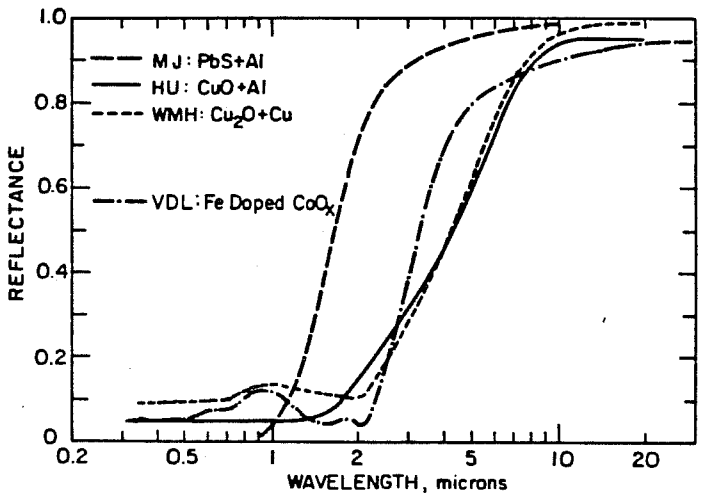

Fig. 15. Reflectance of various tandem absorbers: PbS/Al [57], CuO/Al [58], Cu_2O/Cu [59], CoO_x: Fe/Ni [15].

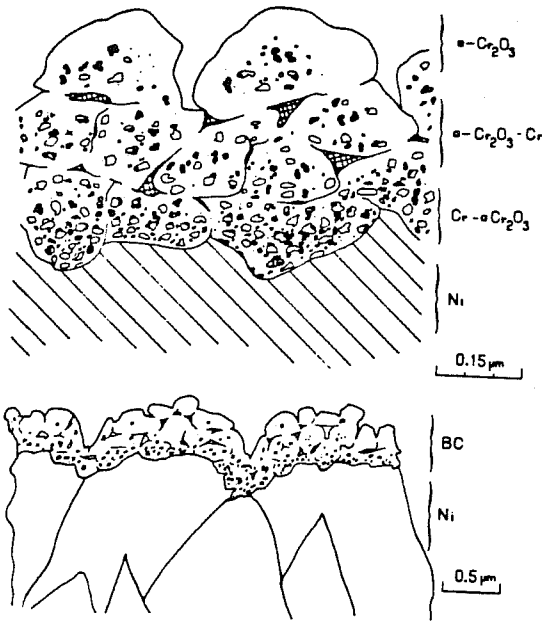

Fig. 16. Schematic cross section of black chrome [62]. Three distinct regions are shown in the as-plated structure: 1. Top layer of amorphous or fine crystalline Cr_2O_3. 2. Intermediate area of metallic Cr in Cr_2O_3. 3. Bottom layers, consisting principally of Cr and Ni substrate.

[39, 44, 55]. The spectral characteristics of black chrome and Cr–Cr_2O_3 cermet coatings are shown in Fig. 17.

Electrodeposited black nickel has a very interesting structure. By changing plating parameters during deposition, layers of ZnS and NiS can be formed on top of a metallic substrate. This absorber shows a combination of tandem and multilayer interference effects. The reflectance for the two varieties is shown in Fig. 18. Multilayer effects will be discussed in a subsequent section. It is important to note that in a number of cases, combined effects in a single absorber may make a superior design, although a more complicated one.

Of theoretical interest regarding tandem absorbers is the theory of Quantum Size Effects (QSE) [69]. QSE occurs in thin film for metals, perhaps less than 10–20 Å for metals and 500 Å for degenerate semiconductors. QSE relates the influence of the geometrical dimensions of the sample to that of distribution of electron states. This distribution can be optimized by size effects to interact strongly with incident electromagnetic radiation. A combination of a QSE material and a reflector metal layer can result in a tandem absorber. QSE has been experimentally verified for InSb/Al, and InSb/Ag [69].

Two effective-medium theories that can be used to describe composite solar absorbers are the Maxwell–Garnett theory [70, 71] and the Bruggerman theory [72].

A novel graded index coating has been devised by DC anodization of aluminum [36]. The coating is made by phosphoric acid anodization followed by an AC electrolysis of a nickel pigmenting bath. The structure of this coating consists of porous Al_2O_3 with the lower portion of the pores filled with bundles of needle-shaped nickel particles. A thin Al_2O_3 barrier layer protects the aluminum substrate. A spectral plot of this absorber is shown in Fig. 19.

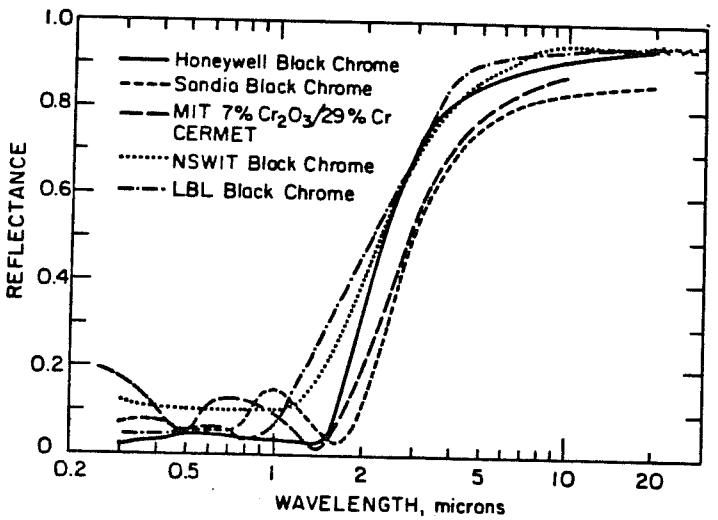

Fig. 17. Reflectance for different types of selective black chrome absorbers [1, 65, 66].

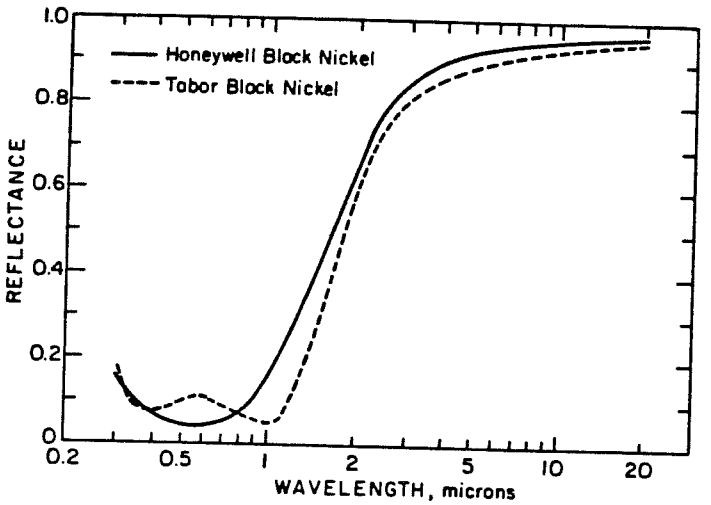

Fig. 18. Spectral reflectance for black nickel [67, 68].

Maxwell–Garnett theory

The Maxwell–Garnett theory (MG) is employed to help elucidate the absorption properties of extremely fine particles in a solid matrix. The MG theory was developed from Mie scattering theory, which describes the scattering properties of spherical particles larger than those that could be handled by the Rayleigh theory. The original MG theory treated isolated spherical metal particles in a dielectric matrix. Also, it was assumed that the particles exhibited identical properties to the bulk metal, which is oversimplified. The MG theory was further developed to take a random distribution of particles characterized by a metal filling factor (f) and simple particle shapes [60, 73]. The diameter (d) of the particles is small compared to the film dimensions and wavelengths (2), so $d < 0.1\lambda$.

Historically, the MG theory has been used to describe the color obtained from colloidal suspension of metal in glass, and it is currently used to predict the properties of uniform ultrafine particulate solar absorbers [73].

In general, a homogeneous isotropic material is optically characterized when the refractive index and the extinction coefficient are known as a function of all wavelengths of interest.

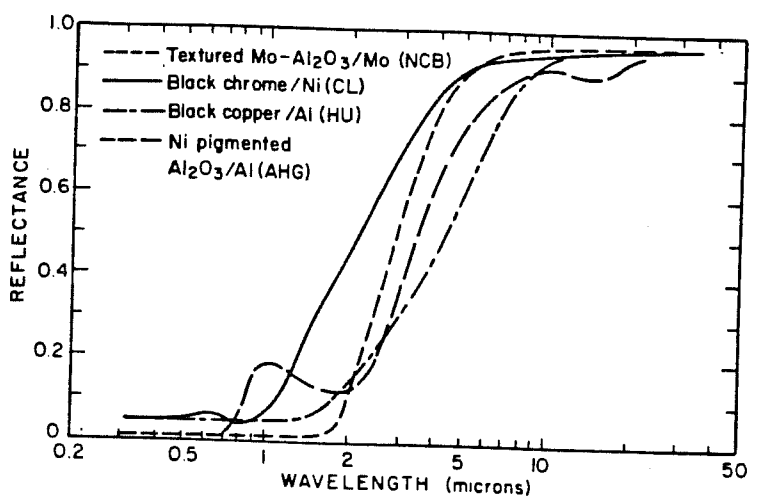

Fig. 19. Spectral reflectance of nickel-pigmented Al_2O_3 absorber [36] shown with textured Mo–Al_2O_3/Mo surface [54], black chrome [62], and copper [58].

Consider a medium composed of metal spheres suspended in a vacuum. There are N spheres per unit volume. Each sphere behaves like an electric dipole with dipole moment P in an applied external field $\bar{E}$. The external field is the sum of the internal field due to the incident light or energy $\bar{E}_i$ plus contributions from other dipoles $\bar{P}$, as expressed in the following relationships:

$$\bar{E} = \bar{E}_i + \frac{1}{3e_0}\bar{P}, \quad \bar{P} = Np = Na\bar{E}_i,$$

where a is the polarizability and e_0 is the dielectric constant of vacuum. The dielectric constant is defined as:

$$e = \frac{e_0\bar{E}+\bar{P}}{e_0\bar{E}} = e_1 + ie_2.$$

Then the dielectric constant can be related to the polarizability by:

$$\left(\frac{e-1}{e+2}\right) = \frac{1}{3e_0}Na.$$

The optical properties should be discussed in terms of a spatially averaged dielectric constant for large wavelengths relative to particle size:

$$\bar{e} = \bar{e}_1 + i\bar{e}_2.$$

To use the Maxwell–Garnett theory, the fill factor of metal to matrix ratio must be $\leqslant 0.2$. Otherwise, corrections have to be made for retardation effects. The Maxwell–Garnett theory gives:

$$\bar{e} = e_d\frac{1+\frac{2}{3}fa}{1-\frac{1}{3}fa},$$

where a is the polarizability factor; for metal spherical particles in a dielectric matrix:
where,

$$a = \frac{(e_m - e_d)}{e_d + Q(e_m - e_d)}, \quad Q = \frac{1}{3},$$

e_m = the complex dielectric constant for the metal,
e_d = the dielectric constant for the oxide, and
Q = the total depolarization factor.

Also $\bar{e}$ can be expressed as:

$$\bar{e} = \frac{e_d[2e_d(1-f)+e_m(2f+1)]}{e_d(f+2)+e_m(1-f)}.$$

The above equation can be expressed in its symmetric form:

$$\left[\frac{\bar{e}-e_d}{\bar{e}+2e_d}\right] = f\left[\frac{e_m-e_d}{e_m+2e_d}\right].$$

Bruggeman effective-medium theory

In the Bruggeman theory (BR) an inhomogeneous two-phase material is treated as a system of spherical particles. These particles are composed separately of pure phase A and pure phase B. The theory solves for the local electric field around a typical two-phase element, embedded in an effective medium. In the BR theory, first-order scattering shall vanish on average; that is, all field fluctuations will average to zero. In this fashion, a self-consistent local field is equivalent to the choice of an active medium such that the average single site scattering is zero. Considering a metal-oxide system, the effective medium dielectric constant results as:

$$\bar{e} = e_d\frac{(1-f+\frac{1}{3}fa)}{(1-f-\frac{2}{3}fa)},$$

where a for spheres is:

$$a = \frac{(e_m-\bar{e})}{\bar{e}+\frac{1}{3}(e_m-\bar{e})},$$

and

e_d = dielectric constant for the oxide,
e_m = dielectric constant for the metal,
$\bar{e}$ = effective dielectric constant,
f = metal fill factor.

Also, the above expression can be seen in its symmetric form:

$$f\left[\frac{e_m-\bar{e}}{e_m+2\bar{e}}\right] = (f-1)\left[\frac{e_d-\bar{e}}{e_d+2\bar{e}}\right].$$

Effective medium bound theory

A range of effective medium theories, including various microstructured shape effects in cermet systems, can be bounded by mathematical theory. An effective dielectric function within bounds can be calculated with knowledge of separate dielectric functions only for phase A and B volume fractions. This can be done regardless of their geometrical configuration [74–76]. The bounds can be developed using the function $F(s)$, which is defined as [75]:

$$F(s) \equiv (e_d - \bar{e})/e_d$$

and

$$s \equiv e_d/(e_d - e_m).$$

The bounds can be derived using the parameteric representation, as [74–75]:

$$F_e(s) = \frac{f(s-s_o)}{s[s-s_o-\frac{1}{3}(1-f)]} \quad \text{for} \quad 0 < s_o < \tfrac{2}{3}$$

and

$$F_f(s) = \frac{f(s-s_o)}{(s-s_o)(s-\frac{1}{3}f)-\frac{2}{3}(1-f)(1-s_o)}$$

for $\frac{2}{3} < s_o < 1$.

Both $F_e(s)$ and $F_f(s)$ represent arcs that intersect on the complex F plane. The area bounded represents allowed values of $\tilde{e}$. Their intersection points are exactly the MG theory result. If percolation is considered for the metal (or phase A), then $F_f(s)$ becomes [76]:

$$F_{fa}(s) = \frac{1}{s}\frac{f(s-s_o)(s-\frac{2}{3})-fs_o(1-s_o)/3(1-2s_o)}{(s-s_o)(s-1+f/3)-fs_o(1-s_o)/3(1-2s_o)}$$

for $0 < s_o < \frac{1}{3}$.

If the dielectric (or phase B) percolates, then $F_f(s)$ becomes:

$$F_{fb}(s) = \frac{f(s-s_o)}{(s-s_o)(s-\frac{1}{3}(1-f))-(1-f)s_o(1-s_o)/3(2s_o-1)}$$

for $\frac{2}{3} < s_o < 1$.

Graphical representations showing the relationship between these bounds and various effective medium theories are detailed elsewhere [76].

Multilayer absorbers

Multilayer thin films can make excellent solar absorbers. Dielectric/metal/dielectric combinations known as interference stacks behave like selective filters for energy absorption. The desired effect of an interference stack is to capture energy between metal–dielectric alternations. Specific solar wavelengths are absorbed by multiple reflection in the layers. Other wavelengths not of the absorption or tuning frequency of the multilayer films are reflected. For solar energy absorption a broadband filter is required. Thin films are generally produced by CVD or PVD processes. Examples of film responses are shown in Fig. 20. The disadvantage with most multilayer coatings is that they are fairly expensive to fabricate compared to a single-layer process. These coatings can also suffer from interdiffusion and corrosion at elevated temperatures and humidity. In spite of all this, stable multilayer coatings do exist, like that of the $Al_2O_3/Mo/Al_2O_3$ design [77]. The metal layer in these coatings is typically 50–100 Å thick to appear semi-transparent to incoming radiation. The dielectric layers need not be intrinsically absorbing to solar radiation since this three-layer structure behaves as a resonant cavity tuned to a band of solar wavelengths. A novel multilayer coating has been devised by DC

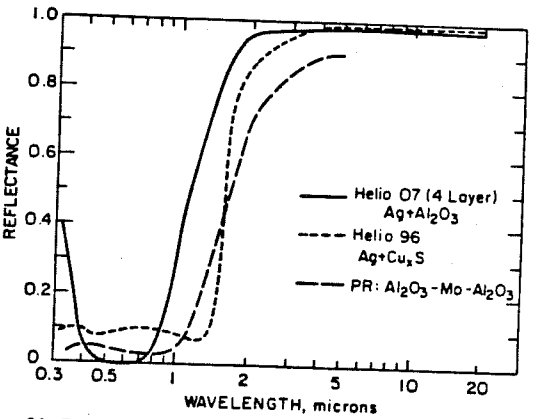

Fig. 20. Reflectance for sample multilayer absorbers of the dielectric/metal type. Also included is the Al_2O_3–Mo–Al_2O_3 high-temperature absorber [77].

anodization of aluminum [36]. The coating is made by phosphoric acid anodization followed by an AC electrolysis of a nickel pigmenting bath. The structure of this coating consists of porous Al_2O_3 with the lower portion of the pores filled with bundles of needle-shaped nickel particles. A thin Al_2O_3 barrier layer protects the aluminum substrate.

Absorber paints

If a thermally resistant, property stable paint could be developed that offered the solar selectivity of black chrome for a low cost, the solar coating industry would be revolutionized. Up to this time a highly selective paint does not exist. There are a few that exhibit partial solar selectivity and are commercially available. Others, however, are still in the research stage. Some properties of selective paints are shown in Table 4. Three approaches can be taken in designing a selective paint. One makes the paint coating very thin so the low infrared emittance of the metal substrate dominates the infrared. Notice that a metal substrate is specified. For passive applications such as Trombe walls the substrate would probably be concrete or brick and this type of paint would be selective. The major problem with thickness-sensitive paints is their binder material. This is usually a polymer, which exhibits dominant infrared-absorption bands. This absorption increases the infrared emittances of the paint. To remedy this either a special polymer must be devised or an inorganic system must be used. Another approach to the paint is to use a coated metal flake in the composition. In this way the selective effect is created as a distributed tandem, with each particle serving as an individual tandem absorber; recent research has documented this effect

Table 4. Selective absorber paints

Type	Highest operating temp. in air	$A_s(T)/E_{ir}(T)$	Ref.
Soot, polyurethane alkyl	>70–100°C	0.90, 0.30 (100°C)	[78]
Thurmalox silicone based	537°C	0.96, 0.52 (84°C)	Dampney Co. Everett, Massachusetts
Solkote–Hi/Sorb	880°C	0.95, 0.44	Solec Princeton, New Jersey
Fe, Mn, Cu oxides +silicone	200°C	0.9, 0.31 (100°C)	[79]
Fe, Mn, Cu oxides and silicone epoxy	200°C	0.9, 0.31 (100°C)	[79]
Fe, Mn, Cu oxides+* /Al flake and silicone	>600°C	0.91–0.93, 0.8–0.1 (20°C)	[79]

* Thickness insensitive.
All data taken from manufactures' product literature or research reports, accuracy or completeness has not been verified.

[79]. A third approach is to use an intrinsic absorber material such as ZrB_2 and disperse it in a low-absorbing binder. The final concept relies upon the development of both the intrinsic absorber and binder.

RADIATIVE COOLING MATERIALS

The earth naturally cools itself by radiative transfer through high-transmission windows in the atmosphere to the cold troposphere. This effect is most noticeable on clear nights. A significant atmospheric window occurs from 8–13 μm wavelength, as shown in Fig. 21. One could conceivably design an upward-facing surface that would emit over this wavelength range [81–89]. To model radiative cooling one must first consider a surface radiating towards the sky. A simplified radiation balance can be used to determine idealized radiative cooling power in the absence of convective and conductive heat-transfer effects [81]. The radiative cooling power (P) is given by:

$$P = bE_s(T_s^4 - T_a^4) + E_{sc}(1 - E_{ac}) \int_8^{13} B_w(T_a)\,dw$$

where:

w = wavelength in microns,
E_s = hemispherical emittance of the cooling surface,
b = Stefan Bolzmann constant,
T_s = temperature of the cooling surface,
T_a = temperature of the atmosphere,
E_{ac} = average hemispherical emittance of atmosphere from 8–13 μm,
E_{sc} = average hemispherical emittance of the surface from 8–13 μm.

E_{sc} is given by:

$$E_{sc} = \frac{\int_8^{13} B_w(T_a)E_s\,dw}{\int_8^{13} B_w(T_a)\,dw}.$$

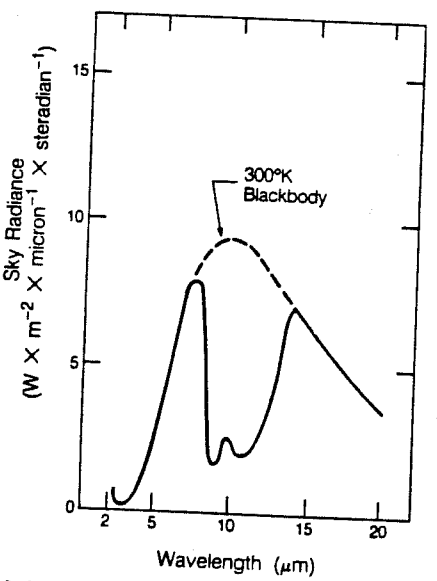

Fig. 21. Infrared spectral sky radiance (solid curve) for clear-sky conditions depicting the atmospheric transparency window at 8–13 μm wavelength [82].

The term E_{ar} can be defined in a similar manner. As a figure of merit the largest cooling-temperature differential requires that E_{sr}/E_s be maximum and that the cooling power at near ambient is governed by E_{sr}.

This implies that a material would have to have high reflectance for 0.3–50 μm, excluding the 8–13 μm region. In the 8–13 μm region the material would have to have a very low reflectance or high emittance. It is theoretically possible for such a surface to reach 50°C below ambient, with typical temperatures about 15°C below ambient. Temperatures below the dew point should be avoided. The cooling power is about < 100 W/m^2 at near ambient.

Solid-state materials used for radiative cooling include SiO/Al, Si_3N_4/Al (see Fig. 22), and polymer-coated metals [81]. Polymers such as polyvinylchloride (PVC), polyvinylfluoride (PVF, Tedlar), and poly-4-methylpentene (TPX) can be used as covers. A radiative-cooling device can also consist of two separate materials, a selective cover and an emitter. Infrared emitters are easier to find, but the selective cover is a challenge. Materials like polyethylene with coatings of Tellurium or dispersions of TiO_2 have been experimented with. Materials need to be designed that not only satisfy the optical requirements but are also resistant to weathering and solar degradation. For the materials investigated this far, the emittance of the coatings needs to be optimized to take full advantage of the 8–13 μm window. Finally, methods of coupling these surfaces with heat-transfer media need to be devised. By using a selectively emitting gas as the emitter, the gas can serve as its own heat transfer medium. Gases such as ammonia, ethylene and ethylene oxide have been investigated [84].

ANTIREFLECTION FILMS

Transparent covers and films used in solar energy conversion systems and architectural windows can have their reflection losses reduced by antireflection treatments. Reflection losses are caused by optical interference from the boundary formed between different media. As a propagating electromagnetic wave in one medium enters another, there is a change in phase velocity, wavelength and direction. Because of interference between the incident wave and the atoms of the new medium, a reflected wave is radiated. This effect is depicted in Fig. 23.

When the incident medium is a vacuum, the ratio of phase velocities (vacuum/medium) is the index of refraction, n. If the medium is energy absorbing, n can be a complex quantity $n = n - ik$. In absorbing media the extinction coefficient k is related to the absorption coefficient $a = 4\pi k/w$, where w is wavelength. Examples of refractive indices (589 nm) of typical media are: air, $n = 1.000393$; water, $n = 1.3336$; crown glass, $n = 1.523$; and diamond, $n = 2.42$. Materials such as window glass ($n = 1.51$) and polymers like polymethyl methacrylate (PMMA), polyvinyl fluoride (PVF), polyethylene terephthalate (PET) poly-

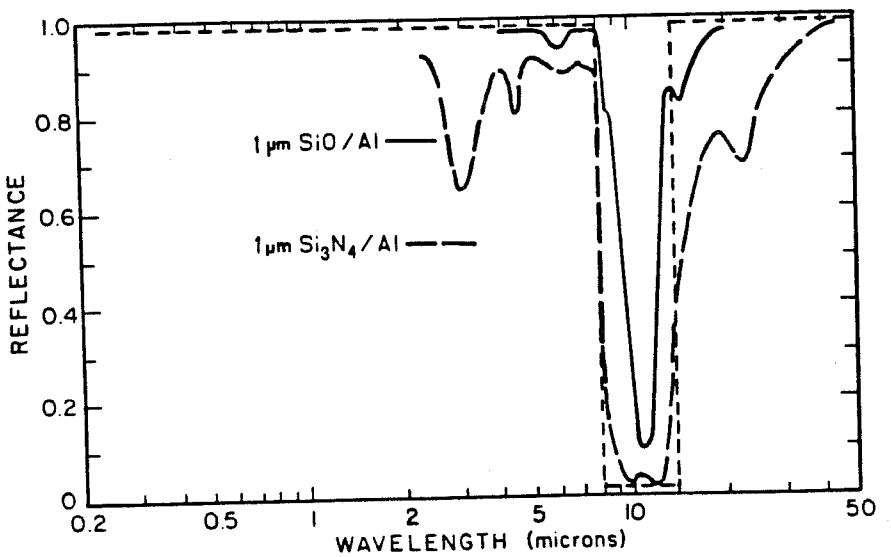

Fig. 22. Spectral properties of radiative-cooling tandems of SiO/Al and Si_3N_4/Al [83]. Ideal properties are shown by the short dashed line.

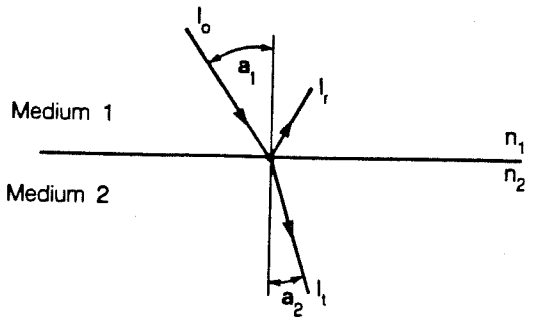

Fig. 23. Angles of incidence and refraction in media having refractive indices of n_1 and n_2.

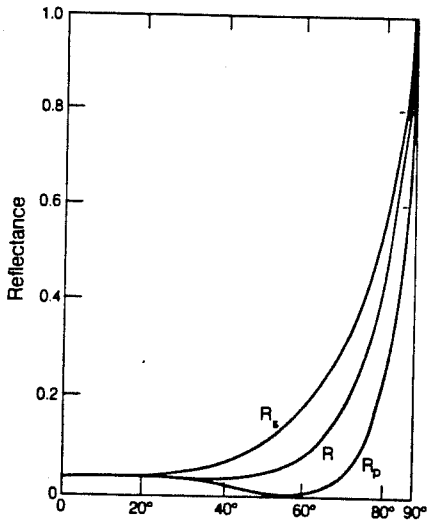

Fig. 24. Dependence of reflectance R, R_p and R_s upon incident angle for air/glass interface.

ethylene and polycarbonate ($n = 1.46-1.54$) are used for solar apertures (see Table 5).

In Fig. 24 the dip in the R_p curve corresponds to the Brewster angle (a_b), which is the maximum polarization in reflection. For glass the Brewster angle is 57° given by:

$$a_b = \tan^{-1}\frac{n_2}{n_1}.$$

At this angle (a_b) p-polarized light is completely transmitted into the medium without reflection. The reason for this effect is that glass partially polarizes (favoring s-polarization) unpolarized incident light by reflection. Also the refracted (transmitted) portion of the beam is partially polarized (favoring p-polarization). At the Brewster angle the electromagnetic vectors for p-polarized light are such that they pass into the glass without interference. Common glare is caused by polarization by reflection and can be supressed by polarizing filters. Several glass sheets or many layers of optical thin films can also produce polarization. One glass plate removes about 8% of light polarized in one direction, and four more plates remove about 67% of polarized light.

The reflectance, R at an interface between two media has been derived by Fresnel as:

$$R = \frac{I_r}{I_o} = \frac{1}{2}\left[\frac{\sin^2(a_2-a_1)}{\sin^2(a_2+a_1)} + \frac{\tan^2(a_2-a_1)}{\tan^2(a_2+a_1)}\right]$$

$$= \frac{1}{2}(R_s + R_p).$$

Non polarized reflectance in this expression is the average of two reflected components of light polarization, R_s perpendicular (s-wave) and R_p parallel (p-

Table 5. Optical properties of transparent cover materials [85]

Material	Index of refraction	Normal incident short-wave transmittance ($\lambda = 0.4$–$2.5\ \mu$)	Normal incident long-wave transmittance ($\lambda = 2.5$–$40\ \mu$)	Thickness (m)
Glass	1.518	0.840	0.020	3.175×10^{-3}
Polymethyl methacrylate (Acrylic, Plexiglass)	1.490	0.900	0.020	3.175×10^{-3}
Polycarbonate (Lexan)	1.586	0.840	0.020	3.175×10^{-3}
Polytetrafluoroethylene (Teflon)	1.343	0.960	0.256	5.080×10^{-5}
Polyvinyl fluoride (Tedlar)	1.460	0.920	0.207	1.016×10^{-4}
Polyethylene teraphthalate (Polyester, Mylar)	1.640	0.870	0.178	1.270×10^{-4}
Polyvinylidene fluoride (Kynar)	1.413	0.930	0.230	1.016×10^{-4}
Polyethylene (Marlex)	1.500	0.920	0.810	1.016×10^{-4}
Fiberglass reinforced polyester (Sunlite)	1.540	0.870	0.076	6.350×10^{-4}

wave). The s-wave electric field oscillates in a plane spatially perpendicular to the plane of incidence. P-waves oscillate in a plane spatially parallel to the plane of incidence. The angles a_1 and a_2 are related to the index of refraction of the non-absorbing media by Snell's law:

$$\frac{n_1}{n_2} = \frac{\sin a_2}{\sin a_1},$$

for absorbing media:

$$\frac{n_1 - ik_1}{n_2 - ik_2} = \frac{\sin a_2}{\sin a_1}.$$

Also, reflectance can be written for nonabsorbing media as:

$$R = \frac{1}{2}\left[\frac{(n_2\cos a_1 - n_1\cos a_2)^2}{(n_2\cos a_1 + n_1\cos a_2)^2} + \frac{(n_2\cos a_2 - n_1\cos a_1)^2}{(n_2\cos a_2 + n_1\cos a_1)^2}\right].$$

For two absorbing media $\bar{n}_1 = n_1 - ik_1$, $\bar{n}_2 = n_2 - ik_2$, then the two reflectance polarizations become:

$$R_s = \left[\frac{(n_2\cos a_1 - n_1\cos a_2)^2 + (k_2\cos a_1 - k_1\cos a_2)^2}{(n_2\cos a_1 + n_1\cos a_2)^2 + (k_2\cos a_1 + k_1\cos a_2)^2}\right],$$

$$R_p = \left[\frac{(n_2\cos a_2 - n_1\cos a_1)^2 + (k_2\cos a_2 - k_1\cos a_1)^2}{(n_2\cos a_2 + n_1\cos a_1)^2 + (k_2\cos a_2 + k_1\cos a_1)^2}\right],$$

and

$$\frac{\sin a_2}{\sin a_1} = \frac{n_1 - ik_1}{n_2 - ik_2}.$$

If reflectance is plotted as a function of incident angle a_1 for a hypothetical air-to-glass ($n = 1.52$) interface, the relationships between R, R_s and R_p can be noted, as shown in Fig. 24.

For radiation at normal incidence $a_1 = a_2 = 0$, so the reflectance equation becomes normal reflectance, R_n:

$$R_n = \frac{(n_2 - n_1)^2}{(n_2 + n_1)^2}$$

and for two isotropic absorbing media the normal reflectance is:

$$R_n = \left[\frac{(n_2 - n_1)^2 + (k_2 - k_1)^2}{(n_2 + n_1)^2 + (k_2 + k_1)^2}\right].$$

So for most polymers and glasses for solar use, other than low-index halocarbons the normal incidence reflectance losses are about 3.5–4.5% per surface. The net increase in performance for each aperture cover would be about 7–9% maximum. This gain in transmittance can be very significant when multiple glazings are used, as demonstrated in Fig. 25.

Now consider the addition of an antireflection layer to the cover surface. In order that two beams annul each other, two conditions must be satisfied: (1) the amplitudes must be equal; (2) the phase difference must be 180°. Consider the situation for isotropic nonabsorbing media at normal incidence. Let n_0 be the refractive index of air, n_1 be the refractive index of the coating and n_2 the refractive index of the substrate. The amplitudes will be equal if the reflectance from the air/coating interface is equal to the reflectance from the coating/substrate interface:

$$\frac{\left(\frac{n_1}{n_0}\right) - 1}{\left(\frac{n_1}{n_0}\right) + 1} = \frac{\left(\frac{n_2}{n_1}\right) - 1}{\left(\frac{n_2}{n_1}\right) + 1},$$

and when $n_1 = (n_2)^{1/2}$ this condition is satisfied. The phase change takes place in the coating for both waves. To produce a phase difference of 180° it is necessary that the phase length be equal to multiples (N) of $\pi/4$ or $2n_1 t = (2N+1)1/2\pi$. Generally no suitable solid material exists with $n_1 = 1.225$ for antireflection of a $n_2 = 1.5$ substrate.

At normal incidence the reflectance is given as:

$$R_n = \left[\frac{n_0 n_2 - n_1^2}{n_0 n_2 + n_1^2}\right]^2.$$

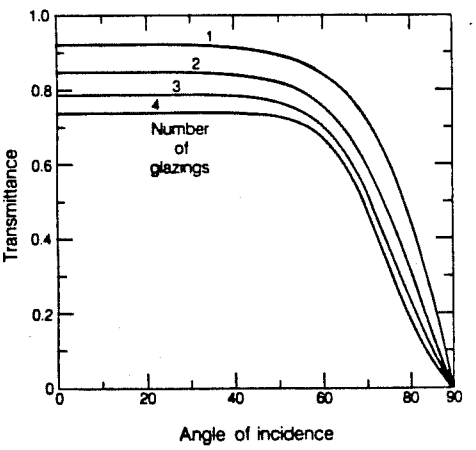

Fig. 25. The idealized transmittance of different numbers of covers showing the effect of reflectance only (no absorption) for a medium with $n = 1.52$.

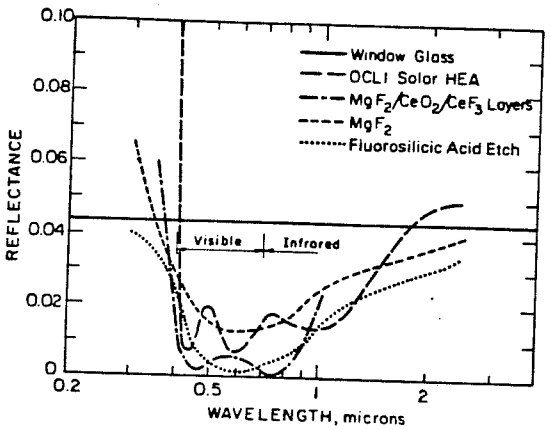

Fig. 26. Specular reflectance for a number of antireflection treatments on glass [1]

Formulas for multilayer films are given elsewhere [6].

Antireflective coatings, if designed properly, can also serve as durable overcoating materials. For photovoltaics, some polymeric and elastomeric protective coatings can be effective antireflective materials if the coating is thin enough, although protective coatings are generally used in thick-film form. Popular protective materials are silicones, fluorocarbons, halocarbons, and acrylic resins. One major need is to develop a coating that serves both protective and antireflective functions. Some polymers having a low refractive index (n) can antireflect glass ($n = 1.5$) and other high-index plastics. Dispersions of fluorinated ethylene propylene ($n = 1.34$) can be used for this purpose. Polyvinyl fluoride ($n = 1.46$) can be antireflected by dipping in acetophenon. Graded-index films present a versatile range of coatings having refractive indices that are not readily found. Fluorosilicic acid can give a graded-index, antireflective coating to glass (see Fig. 26). It primarily roughens the surface by etching out small pores, in non-silica regions [86, 87]. Silica films deposited from sodium silicate or collodial silica can be used for acrylic, polycarbonate, and several glasses. A treatment for polyethylene terephthalate (polyester) and glass materials has been devised [88, 89]. The coating is made from a steam-oxidized aluminum film; this processing causes a needle-like structure of aluminum hydroxide [AlO(OH)] to form. A polyester film treated in this fashion can serve in glazing applications where solar transmission must be optimum [90] (see Fig. 27). Inorganic thin films have been used for a wide range of single and multiple interference-coating applications. Compounds such as MgF_2, CeO_2, SiO, SiO_2, and TiO_2 in various combinations have been used for antireflection applications. Other than the traditional PVD techniques, a number of oxides can be dip-coated onto optical substrates. Coatings of hot hydrolyzed metal alkoxides can be polycondensed, forming oxides of transition metals, refractory metals, and some rare earths [91]. A similar technique known as the sol-gel process has formed mixed TiO_2–SiO_2 antireflective films on silicon [92] and black chrome. Diamond-like (i-carbon) transparent coatings have been used for antireflective films. They are formed from plasma decomposition by hydrocarbons and ion beam deposition [93]. Coatings of about $n = 1.9$ can

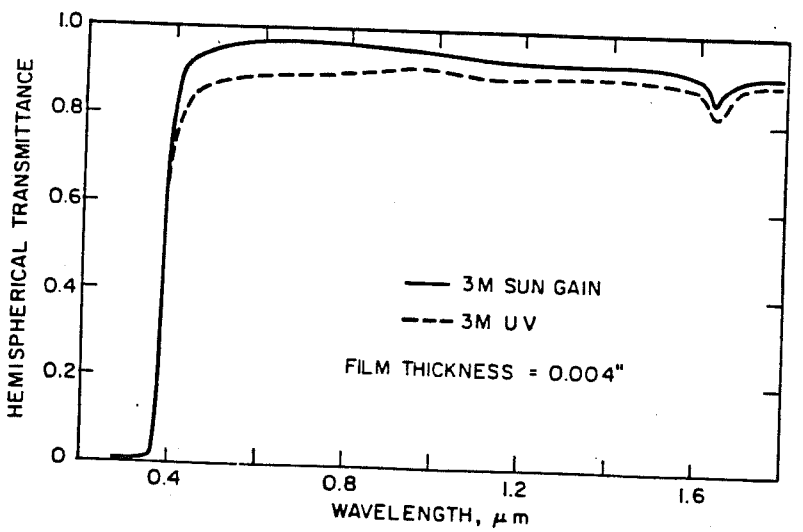

Fig. 27. Hemispherical transmission of antireflected 3M Sungain polyester film compared to the uncoated substrate [84].

be made that are suited to photovoltaics. However, the absorption properties of i-carbon films must be reduced before they can be utilized for optical applications.

REFLECTOR MATERIALS

Reflector materials consist of a metal reflector on a substrate either in a front-surface or back-surface configuration. They can differ according to the method of metallic deposition, be it either silver, aluminum or an alloy reflector. The substrate material can be flexible or rigid.

Front-surface mirrors offer the best initial optical reflectance but suffer from abrasion and atmospheric corrosion and delamination. Application of a durable overcoating material is required. Second-surface mirrors are conventionally produced by a wet chemical process. For mirrors made with this process, there is considerable lack of understanding of various interfacial reactions and degradation mechanisms that can occur with time. A recent workshop addressed many of these investigated [94]. Also, more durable reflector layers for second-surface mirrors have been devised by sputtering, evaporation, and decomposition of organometallic resinates [95]. For both types of reflectors an understanding of the stability between metal/polymer and metal/glass mirrors is a significant issue. Dirt and dust can be responsible for considerable decline of efficiency of reflector surfaces. Techniques to limit dusting and washing of surfaces need to be devised.

Due to the variety of solar applications for reflector material, the optical requirements for solar mirrors vary greatly, but all are sensitive to the integrated solar reflectance. The spatial distribution of reflected light from a mirror surface is another important parameter since a mirror can range from highly diffuse to highly specular. The amount of this spatial variation is known as specularity. Specularity is dependent upon the exact roughness and contour variations of the mirror surface. Ranges of specularity are shown in Fig. 28.

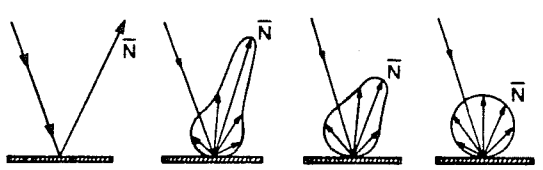

Fig. 28. Angular light distribution in ideal specular reflection (left) and total diffuse reflection (right).

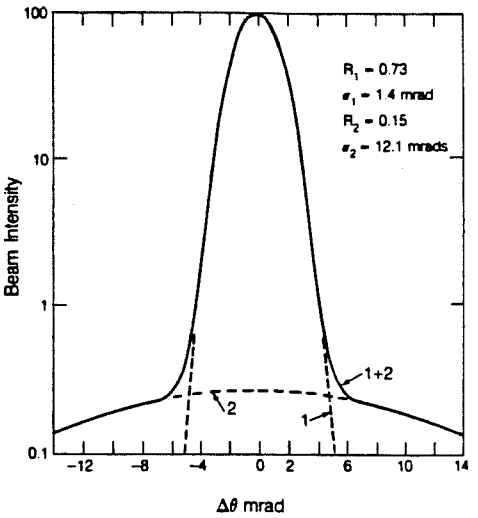

Fig. 29. Reflected beam profile for aluminized teflon film at 400 nm as a function of angular aperture (after Ref. [96]).

The normal clear-day distribution of direct solar beam radiation has a normal distribution and dispersion of $d_s = 3.5$ milliradians (mrad). The effective dispersion d_e after reflection from a mirror with dispersion d_m is given by:

$$d_e = [d_s^2 + d_m^2]^{1/2}.$$

The dispersion for the mirror surface is measured on a bidirectional reflectometer with a variable collection slit [96]. An example beam profile is shown in Fig. 29.

The specular reflectance properties for several mirror materials are shown in Fig. 30 and Table 6.

FLUORESCENT CONCENTRATORS

Fluorescent materials can be used to down-convert or alter spectrally incident radiation, and to concentrate and guide it along the plane of the material. This process is shown schematically in Fig. 31. A fluorescent concentrator consists of a transparent plate (of polymer or glass) that has been doped with fluorescent dye molecules. Depending upon the dyes used, various spectral compositions can be obtained. A combination of coupled dyes is depicted in Fig. 32. Incident light corresponding to the fluorescent absorption of the dye will be captured and emitted isotropically. Because of the index of refraction difference between the plate and surrounding medium, a large portion of light will be trapped and guided to the edges of the plate by total internal reflection. One edge can be favored by silvering the other three edges (see Fig. 31). At this favored edge a photovoltaic or

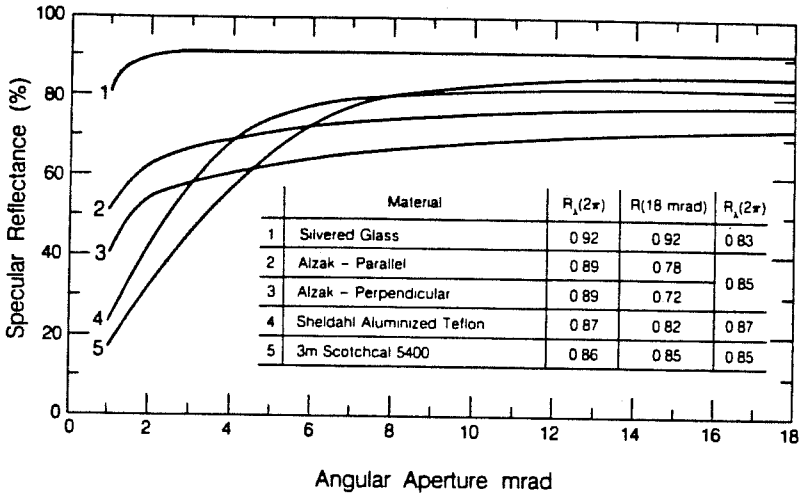

	Material	$R_\lambda(2\pi)$	R(18 mrad)	$R_\lambda(2\pi)$
1	Silvered Glass	0 92	0 92	0 83
2	Alzak – Parallel	0 89	0 78	0 85
3	Alzak – Perpendicular	0 89	0 72	
4	Sheldahl Aluminized Teflon	0 87	0 82	0 87
5	3m Scotchcal 5400	0 86	0 85	0 85

Fig. 30. Specular reflectance properties for several solar mirror materials. The inset table lists hemispherical reflectance R_n, integrated specular solar reflectance R_s, and specular reflectance at 18 milliradians [96].

photothermal collector can be placed [98–102]. One of the unique advantages of this system is that it will collect diffuse, low-insolation radiation without solar tracking. Other advantages are that there is less heat dissipation in photovoltaics and high efficiency at low insolation levels. Concentration ratios for these systems can be fairly high (10–100). The collection efficiency of this system is dependent upon a number of factors. The loss due to light leaving the collector through the boundary planes by fluorescence for a single plate is given by:

$$L = \frac{1-(n^2-1)^{1/2}}{n},$$

where n is the index of refraction of the collector plate. If $n = 1.5$, then $L = 0.255$; if $n = 2$, then $L = 0.134$. This equation implies that n should be as large as possible to minimize loss. But another process is important, that of external reflection loss which implies a low n. This loss is given by the Fresnel equation. As a result, the total optical loss of the system is given by:

$$L_T = \frac{1-4(n^2-1)^{1/2}}{(n+1)^2}.$$

A minimum occurs at $n = 2.0$, $L_T = 0.23$. If we consider the role of the dye and its associated properties, then an overall concentrator efficiency (n_c) can be derived:

$$n_c = n_q n_f n_g n_c n_s,$$

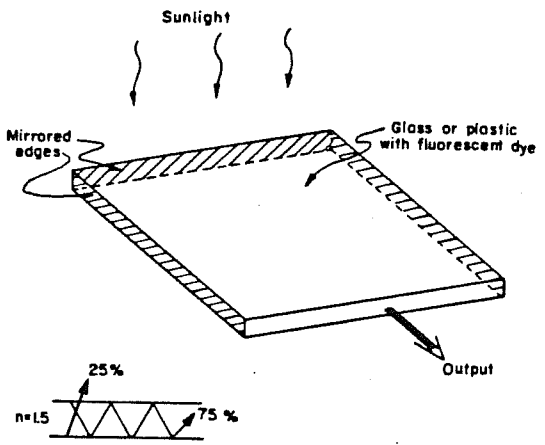

Fig. 31. Schematic representation of a fluorescent concentrator showing how light can be guided along the plane of the material.

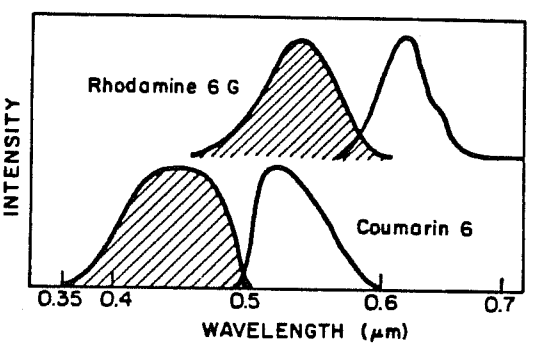

Fig. 32. Spectra of coupled fluorescent dyes. Absorption wavelengths are crosshatched. Emission spectra are shown spectrally downshifted.

Table 6. Specular reflectance properties of mirror materials [97]

Material	Supplier	Estimates of solar weighted reflectance* at receiver acceptance angle τ $\tau = 4$ mr	10 mr	18 mr	$R_s(2\pi)$
I. Second-Surface Glass					
(a) Laminated Float Glass-2.7 mm thick-silvered	Carolina Mirror Co.	0.83	0.83	0.83	0.83
(b) Laminated Low-Iron Sheet Glass-3.35 mm thick-silvered	Gardner Mirror Co.	0.90	0.90	0.90	0.90
(c) Corning Silvered Microsheet Co. −0.114 mm thick-mounted on optically flat plate	Corning Glass	0.76	0.87	0.92	0.95
(d) Corning 0317 glass-1.5 mm thick-evaporated silver	Corning Glass	0.95	0.95	0.95	0.95
II. Metallized plastic films					
(a) 3M Scotchcal 5400 Laminated to backing sheet	3M Company	0.60	0.84	0.85	0.85
(b) 3M FEK-163 Laminated to backing sheet	3M Company	0.83	0.85	0.85	0.85
(c) Aluminized 2 mil FEP Teflon (G405600) Laminated to backing sheet	Sheldahl	0.70	0.81	0.82	0.87
(d) Silvered 2 mil FEP Teflon (G400300) Mounted on optically flat plate	Sheldahl†	0.73	0.82	0.90	0.96
(e) Silvered 5 mil FEP Teflon (G401500) Mounted on optically flat plate	Sheldahl†	0.77	0.83	0.89	0.95
(f) Front surface aluminized Mylar (200XM648A) stretched membrane	Boeing	0.88	0.88	0.88	0.88
III. Polished, bulk aluminum					
(a) Alzak Type I specular	Alcoa				0.85
perpendicular to rolling marks		0.61	0.68	0.76	
Parallel to rolling marks					
(b) Kinglux No. C4	Kingston Ind.	0.68	0.76	0.83	0.85
perpendicular to rolling marks					
Parallel to rolling marks		0.67	0.71	0.75	
(c) Type 3002 high purity	Metal Fabrications, Inc.†	0.69	0.71	0.75	0.84
Al—buffed and		0.44	0.60	0.71	
bright anodized					

* Estimated from 500 nm specularity data (Ref. [96]) and solar weighted total hemispherical reflectance data. Standard deviation of the estimates is about 2% (1 mr = 0.0573°).
† Experimental materials not produced in high production.

where n_q is defined as the quantum efficiency of the fluorescent dye; n_f is the efficiency due to fluorescent emission beyond the limiting angle of total internal reflection; n_g is the efficiency due to collector geometry (absorption); n_e is the energy conversion efficiency due to the Stokes wavelength shift associated with fluorescence and finally, n_s is the loss of the long- and short-wavelength tails of the solar spectrum. For thermal collectors fluorescent concentrators, operational efficiencies of 42–59% have been estimated. For photovoltaic systems, operating efficiencies of 32% for a four-glazing plate system have been estimated [98]. By using multiple plates various portions of the solar spectrum can be collected. Each level of collector plate down has a higher absorption energy, so that the innermost level absorbs the highest solar energy. A backup mirror is used on the lowest level to reflect unused energy to the upper lower-energy fluorescent levels. This action is seen in Fig. 33.

Current research on fluorescent concentrators has

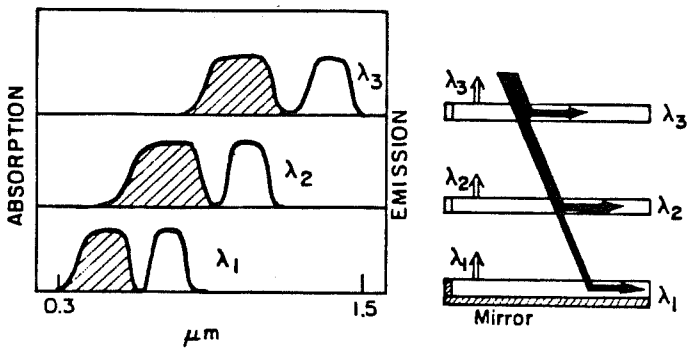

Fig. 33. Three-stage fluorescent concentrator depicting peak wavelengths for each stage.

favored polymethyl methacralate (PMMA) and rare-earth-doped glasses as host materials for the dye [99–103]. Their high optical transmission property is good to about 1 μm wavelength. For a variety of glazing uses there is a need to devise durable glazing materials that can maintain transparency further into the infrared. Dyes that are used for experimentation have not been specifically tailored for solar uses. Experimental collectors generally use laser dyes. Dyes need to be developed with high quantum efficiency, with separated emission spectra with low self-absorption. One of the most severe requirements for the dyes is that they be UV stable in the PMMA matrix. It is possible that new materials such as ligands containing rare earth ions and nonradiative coupled organic systems may offer greater stability. Furthermore, it may be possible to make a polymer-based fluorescent thin film that, by index matching, could couple energy into a substrate material. This design could minimize reabsorption by the dye. Emission–absorption coupled dyes may offer a wide variety of solar collection and energy redistribution possibilities.

SPECTRAL SPLITTING AND COLD MIRROR FILMS

Spectral splitting coatings are used to divide the solar spectrum into various broadband regions. In this fashion, various regions can be tailored to particular photovoltaic or photothermal needs [104–106]. A simple design utilizing a heat mirror might be used to separate heat and light from the solar spectrum. The infrared energy could be used for photothermal uses and the high energy visible could be used for a photovoltaic. Photovoltaics will operate more efficiently if infrared heating is eliminated. Expanding this idea further, a system depicted in Fig. 34 could result, for an all-photovoltaic system. If heat mirrors with different spectral characteristics were used, the solar spectrum could be partitioned from low to high energy as the heat mirror transition wavelength becomes shorter. Broadband Lippmann holograms can also be used for spectral splitting [106].

A coating known as a cold mirror could also be employed for spectral splitting. A system might consist of a series of cold mirrors, where the transition from reflecting to transmitting moves to longer wavelengths for each successive cell, as shown in Fig. 34. The cold mirror has the opposite spectral response to that of the heat mirror. It exhibits high reflectance in the visible region and transmits highly in the infrared.

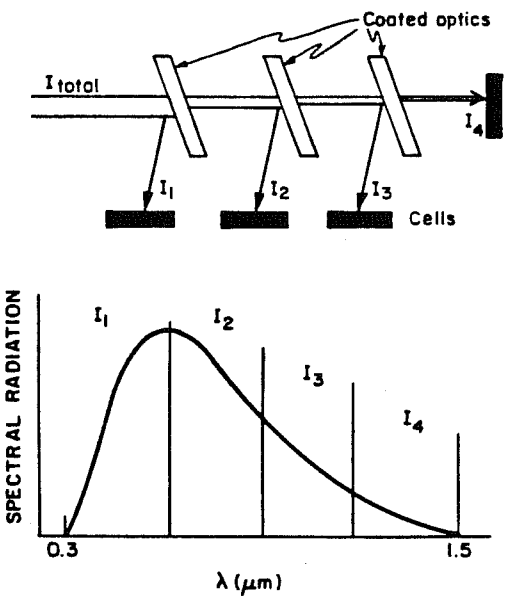

Fig. 34. Spectral splitting scheme for photovoltaics.

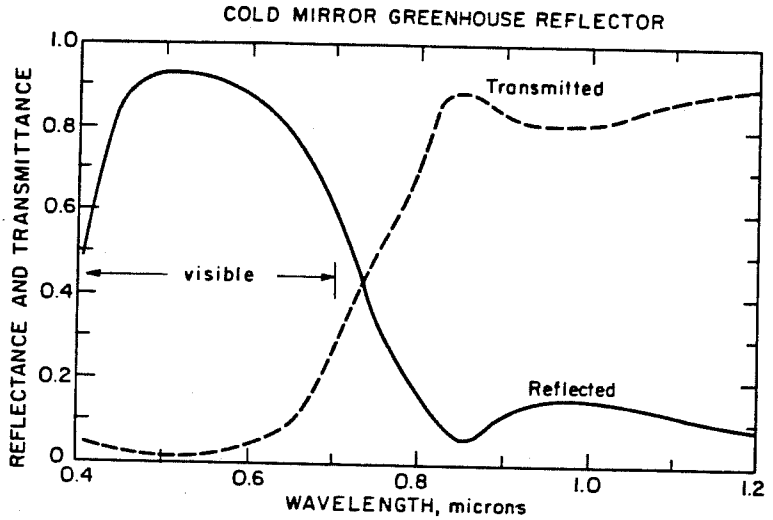

Fig. 35. Cold mirror coating for greenhouse baffle collector [108].

Cold mirrors are generally all dielectric interference films. Material systems such as ZnS/MgF_2 and TiO_2/SiO_2 have been devised [107–108]. Spectral characteristics of a commercial film are shown in Fig. 35. An application for this film is for greenhouses [108]. Plants require only a range of wavelengths (0.3–0.75 μm); the remainder of the solar spectrum is unused. This remainder can be utilized as heat to warm the greenhouse indirectly. A baffle-type greenhouse is depicted in Fig. 36. Heat mirrors can also be used in this fashion [109].

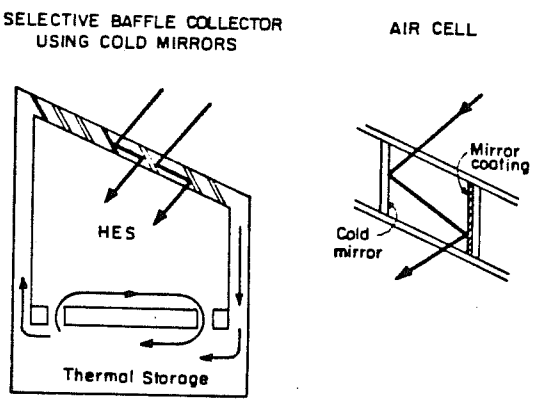

Fig. 36. Selective baffle greenhouse using cold mirror coatings to separate heat from visible energy. The roof is made of air cells that circulate heated air to the thermal storage. In this fashion the solar spectrum is divided to suit both needs without an added collector area.

TRANSPARENT INSULATION MATERIAL

One of the major drawbacks of conventional windows is their high thermal loss characteristics compared to other building elements. As discussed previously, surface treatments and modified window design can do much to solve this shortcoming. Another approach is to develop a highly transparent material that, by virtue of its bulk properties has low thermal conductivity. Research on one such material, known as silica aerogel, has begun [110–112]. This material has a microstructure of bonded fine silica particles surrounded with high porosity volume. Since the particles are smaller than a wavelength of visible light, thery are not visibly scattering. The thermal conductivity of such a material is better than still air with optical properties similar to silica glass except for $n = 1.05$. This material has been modeled optically by the Rayleigh Theory [110]. Silica aerogel is made by producing a colloidal silica gel from hydrolysis and polycondensation reaction. This gel is solidified in place by supercritical drying. The disadvantage of aerogel is that it must be protected from shock and moisture. It is possible to form aerogel between two sheets of glass to make a window. For a window of aerogel (20 mm thick), the thermal conductance (U) is calculated [110] to be about $1 W/m^2 K$ (R-5). For a double glazing without the aerogel (20 mm spacing), $U = 2.8 W/m^2 K$ (R-2). The solar hemispherical transmission properties for aerogel are $T_s = 0.67$ (20 mm thick) and $T_s = 0.9$ (5 mm thick). Examples of optical properties are shown in Fig. 37.

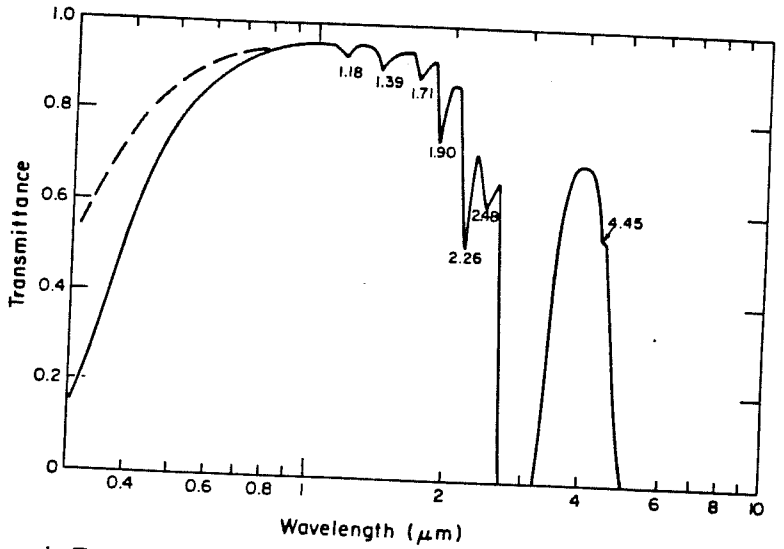

Fig. 37. Example. Transmission properties of 4 mm thick Silicon Aerogel [110]. Spectral normal–normal transmittance (solid line) and spectral normal hemispherical transmittance (dashed line).

OPTICAL SWITCHING MATERIALS AND DEVICES

There are various physical processes that can be used for the regulation of incident solar energy and glare in buildings. Optical switching materials or devices can be used for energy-efficient windows or other passive solar uses. The basic property of an optical shutter is that it offers a radical change in optical properties upon a change in light intensity, spectral composition, heat, electrical field or injected charge. This optical change can be manifested in a transformation from highly transmitting to reflecting either totally or partly over the solar spectrum. The purpose of such a device would be to control the flow of light and/or heat into and out of a building window, according to an energy management scheme. This device could also control lighting and heating levels for energy load functions. In general, the idea of an optical shutter is a scientific possibility based on a future research and design ideas. Phenomena of interest such as optical switching processes, can be classified as either discrete mass movement or collective particle movement. Discrete mass movement includes ion and localized electron motion (photorefractive, chromogenic and redox reactions) and ion and delocalized electron population changes (reversible electrodeposition). Collective particle movement includes gas or vacuum deformable membranes and adjustable diffraction gratings as one category and liquid crystals and electrophoresis processes as another.

Only selected physical processes will be covered here. Chromogenic reactions known as photochromism, thermochromism, and electrochromism will be discussed along with holographic and liquid crystals.

Photochromic materials

Photochromic materials alter their optical properties with light intensity. Generally, photochromic materials are energy-absorptive. Basically, the phenomenon is the reversible change of a single chemical species between two energy states having different absorption spectra. This change in states can be induced by electromagnetic radiation. Photochromic materials have been reviewed [113–115]. Probably the best known photochromic material is photochromic glass for eyeglasses and goggles. Photochromic materials are classified as organics, inorganics, and glasses. Within the organics are stereoisomers, dyes, and polynuclear aromatic hydrocarbons. The inorganics include ZnS, TiO_2, Li_3N, HgI_2, HgCNS, and alkaline earth sulfides and titanates, with many of these compounds requiring traces of heavy metal or a halogen to be photochromic. Glasses that exhibit photochromism are Hackmanite, Ce, and Eu doped glasses (which are ultraviolet sensitive), and silver halide glasses (which include other metal oxides). Of all the photochromic materials the bulk of the information is on the alkali-halide glasses. The silver halide glasses transform by color-center formation from an

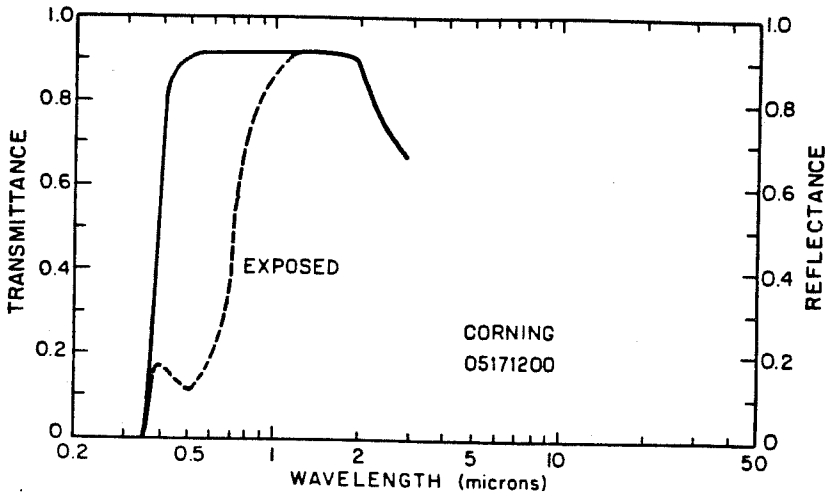

Fig. 38. Sample light and dark transmission spectra for Corning photochromic glass [116].

AgCl crystalline phase. The typical response for a photochromic glass is depicted in Fig. 38. A photochromic plastic has been formulated using derivatives of spiroindolinonaphthoxazine in a matrix of cellulose acetate butyrate and other plastics [117]. This material may have future use for energy regulating glazings for solar energy control.

Thermochromic materials

Many thermochromic materials are used as non-reversible temperature indicators by displaying a color change with temperature variation. For an optical shutter one must consider only the reversible materials, although their actual cyclic lifetime may be dependent on non-reversible secondary reactions. Certain organic compounds in the anil, spiropyrans, polyvinyl acetal resins, and hydrozide groups exhibit thermochromism. Inorganic thermochromic compounds include AgI, HgI_2, Ag_2HgI_4, HgI, $SrTiO_3$, Cd_3P_3Cl, along with various copper, cobalt and tin complexes [118]. Another broad group of materials that exhibit thermochromism are the semiconductor to insulator transition compounds. Examples of these compounds are VO_2, V_2O_3, Ti_2O_3, Ti_4O_7, Ti_5O_9, NbO_2, Fe_3O_4, $FeSi_2$ and NiS [119].

Current research for solar energy application has been on the $V_{1-x}M_xO_2$, (where M is a transition metal) compounds. Such materials, if perfected, can be used to control both the solar transmittance and infrared emittance of a glazing or surface. [120].

Electrochromic materials and devices

Electrochromism is exhibited by a large number of materials both inorganic and organic. The electrochromism effect is of current research interest mainly because of its application to large-scale electronic information display devices, optical switching windows and reflectors for architectural and automotive uses. The electrochromic effect, in essence, is a material that exhibits intense color change due to the formation of a colored compound. The reaction might follow: $MO_x + A^+ + ye \leftrightarrow A_yMO_x$ for cathodic materials.

There are three categories of electrochromic materials: transition metal oxides, organic compounds, and intercalated materials. The materials that have gained the most research interest are WO_3, MoO_3, and IrO_x films. These compounds, among other transition metal oxides, are the subject of a few research reviews [121–123]. Organic electrochromics are based on the liquid viologens, anthraquinones, diphthalocyanines, and tetrathiafulvalenes. With organics, coloration of a liquid is achieved by an oxidation–reduction reaction, which may be coupled with a chemical reaction. Intercalated electrochromics are mostly based on graphite and so are not useful for window applications.

A solid-state window device can be fabricated from five (or less) layers consisting of two transparent conductors (TC), an electrolyte or fast-ion conductor (FIC), counter electrode (CE), and electrochromic layer (EC), as shown in Fig. 39. Much research is needed to develop a usable panel, better electrochromic materials with high cycle lifetimes, and short response times. Certainly fast-ion conductors and solid electrolytes also require study.

Several research groups are investigating electrochromic materials and devices. The most researched materials are amorphous WO_3, crystalline WO_3 and $Ni(OH)_2$. Crystalline WO_3 offers near-infra-

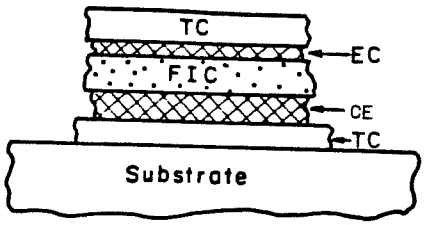

Fig. 39. Schematic structure of a solid-state electrochromic device.

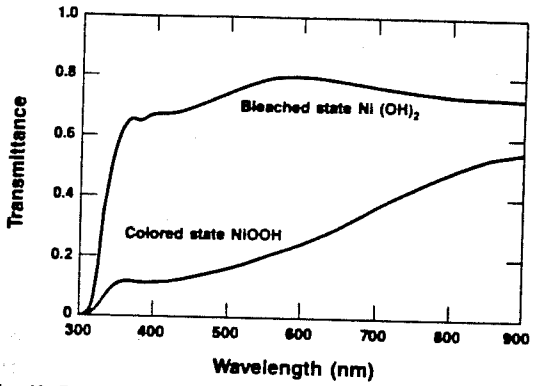

Fig. 40. Spectral transmission of electrochromic nickel oxide film on tin-oxide coated glass substrate. T_v (off) = 0.77 T_v (on) = 0.21. Also solar transmission is T_s (off) = 0.73 and T_s (on) = 0.35. The film was colored by the application of a 1 V pulse at 0.1 Hz.

red modulation, which has the potential to control the infrared portion of the solar spectrum [127–128]. An example of the optical response of electrochromic $Ni(OH)_2$ is shown in Fig. 40 [124–130].

LIQUID CRYSTALS

Thermotropic liquid crystals are actively used for electronic and temperature indicating displays. Liquid crystals exist in one of the three structural mesophases: smectic, nematic and twisted nematic (cholesteric). Chemically, they are based on azo-azoxy esters, biphenyls and Schiff bases [131]. The most widely used type for electronic displays is the twisted nematic type [132]. For optical shutters, the twisted nematic type is not a good choice since it requires polarizers which reduce transmission. The dynamic scattering nematic liquid crystals offer promise as optical shutter materials. In the activated state, the material becomes translucent white. An example of its optical properties is shown in Fig. 41. The switching effect of this device spans the entire solar spectrum, up to the absorption edge of glass. The scattering properties of nematic liquid crystals can be utilized by encapsulating the materials in a polymer matrix of matched optical index. In the off-state, the materials appear translucent white. When activated, the liquid crystal droplets align and the material becomes transparent [133]. Pleochroic dyes can be added to darken the device in the off-state. Liquid crystals can be used as optical filters if they are aligned and solidified by polymerization. This processing can give preset optical properties. In general, the drawbacks of liquid crystals as optical switching materials are cost, limited grey scale and problems in fabricating large area devices (though this is being overcome). Compared to electrochromics, the power consumption is higher due to the need for continuous power in the activated state.

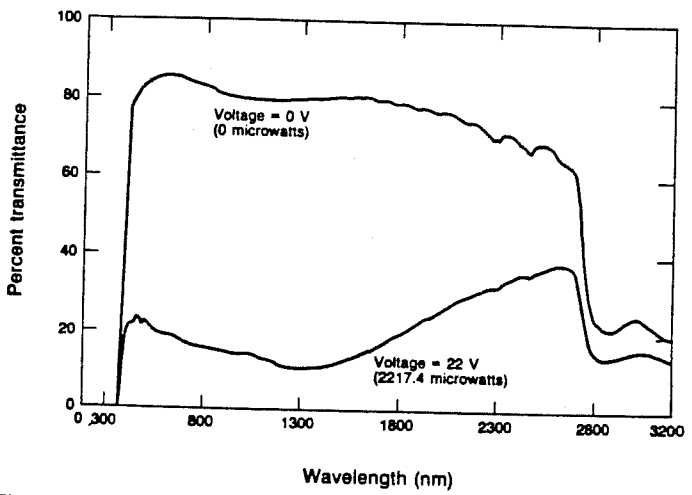

Fig. 41. Spectral transmittance of a dynamic scattering liquid crystal device.

CONCLUSIONS

A very wide range of categories of optical materials have been covered for solar energy and related applications. Attention has been paid to current advances and modern optical materials. Also, the potential for advanced materials (such as optical switching of glazings) has been discussed from a materials science viewpoint. There are still categories of materials that have not been covered here. For example, photovoltaic and photoelectrochemical materials have been excluded. Also, new categories, such as large area light guide materials and holographic films, need to be developed for solar energy applications. In this work it is hoped that by better understanding these optical materials will result in new and improved solar energy conversion devices and systems.

Acknowledgements—This paper was created as the result of educational lectures given at four scientific institutions over the course of several years: Gansu Natural Energy Research Institute, Lanzhou, China, April 1986, The International Center for Theoretical Physics, Trieste, Italy, September 1985, University of Split, Yugoslavia, September 1983 and the International Institute for Advanced Studies, Caracas, Venezuela, June 1982.

This work was supported by the Assistant Secretary for Conservation and Renewable Energy, Office of Building Energy Research and Development, Building Systems Division of the U.S. Department of Energy under Contract No. DE-AC03-76SF00098.

REFERENCES

1. C. M. Lampert, Coatings for enhanced photothermal energy collection, I & II. *Sol. Energy Mat.* **1**, 319 (1979); **2**, 1 (1979).
2. C. M. Lampert, Heat-mirror coatings for energy conserving windows. *Sol. Energy Mat.* **6**, 1 (1981).
3. O. P. Agnihotri and B. K. Gupta, *Solar Selective Surfaces*. Wiley, New York (1981).
4. M. Rubin, R. Creswick and S. Selkowitz, Transparent heat mirrors for windows—thermal performance. *Proc. 5th National Passive Solar Conf.*, pp. 990–994. Pergamon Press, New York (1980).
5. R. M. Winegarner, Heat mirror—a practical alternative to the selective absorber. *Proc. ISES Am. Sect. Sol. Energy Soc. Can.* Pergamon Press, New York (1976).
6. Z. Knitle, *Optics of Thin Films*. Wiley, London (1976).
7. K. Chiba, S. Sobajima, U. Yonemura and N. Suzuki, Transparent heat insulating coatings on polyester film using chemically prepared dielectrics. *Sol. Energy Mat.* **8**, 371 (1983).
8. J. C. Fan, F. Bachner, G. Foley and P. Zavracky, Transparent heat mirror films of TiO_2/Ag/TiO_2 for solar energy collection and radiation insulation. *Appl. Phys. Lett.* **25**, 693 (1974).
9. W. J. King, *High Performance Solar Control Windows*. Lawrence Berkeley Laboratory Report, Berkeley, CA, LBL-12119, U.S.A. (1981).
10. B. P. Levin and P. E. Schumacher, *A Discussion of Heat Mirror Film: Performance, Production Process and Cost Estimates*. Lawrence Berkeley Laboratory Report, Berkeley CA, LBL-7812, U.S.A. (1977).
11. J. Dolenga, Low-E: Piecing together the puzzle. *Glass Magazine*, p. 116 (March 1986).
12. M. M. Koltun and S. A. Faiziev, *Geliotekhnika* **10**, 58 (1974).
13. C. M. Lampert, Materials chemistry and optical properties of transparent conductive thin films for solar energy utilization. *Ind. Engng. Chem. Prod. R&D* **21**, 612 (1982).
14. H. Kostlin, R. Jost, W. Lems, Optical and electrical properties of doped In_2O_3 films. *Phys. Status Sol.* **A29**, 87 (1975).
15. G. Haacke, Evaluation of cadmium stannate films for solar heat collectors. *Appl. Phys. Lett.* **30**, 380 (1977).
16. M. Van der Leij, *Spectral Selective Surfaces for Thermal Conversion of Solar Energy*. Delft University Press, Delft (1979).
17. J. C. C. Fan, Wavelength-selective surfaces for solar energy utilization. *Proc. SPIE* **85**, 39 (1977).
18. R. P. Howson and M. I. Ridge, Heat mirrors on plastic sheet using transparent oxide conducting coatings. *Proc. SPIE* **324**, 16 (1982).
19. K. Itoyma, Properties of Sn-doped indium oxide coatings deposited on polyester film by high rate sputterings. *J. Electrochem. Soc.* **126**, 691 (1979).
20. C. M. Lampert, ed. *Optical coatings for energy efficiency and solar applications. Proc. SPIE*; Vol. 324, The Internal Society for Optical Engineering, Bellingham WA, U.S.A. (1982).
21. V. A. Baum and A. V. Sheklein, Choice of materials for selective transparent insulation. *Geliotekhnika* **4**, 50 (1968).
22. G. Haacke, Transparent conducting oxides. *Ann. Rev. Mat. Sci.* **7**, 73 (1977).
23. J. L. Vossen, Transparent conducting films. In *Physics of Thin Films* (Edited by G. Hass, M. Francombe and R. Hoffman). Academic Press, New York (1977).
24. P. Drude. *Phys. Z.* **1**, 161 (1900).
25. W. F. Bogaerts and C. M. Lampert, Materials for photothermal solar energy conversion. *J. Mat. Sci.* **18**, 2847 (1983).
26. S. A. Herzenberg and R. Silberglitt, Low temperature selective absorber research. *Proc. SPIE* **324**, 92 (1982).
27. B. O. Seraphin, ed., *Solar Energy Conversion-Solid State Aspects*. Springer, Berlin (1979).
28. M. M. Koltun, *Selective Optical Surfaces for Solar Energy Converters*. Allerton Press, New York (1981).
29. A. B. Meinel and M. P. Meinel, *Applied Solar Energy An Introduction*. Addison Wesley, Reading (1976).
30. E. Randich and R. B. Pettit, Solar selective properties and high temperature stability of CVD ZrB_2. *Sol. Energy Mat.* **5**, 425 (1981).
31. G. L. Harding and M. R. Lake, Sputter etched metal solar selective absorbing surfaces for high temperature thermal collectors. *Sol. Energy Mat.* **5**, 445 (1981).
32. C. M. Lampert and J. Washburn, Microstructure of a black chrome solar selective absorber. *Sol. Energy Mat.* **1**, 81 (1979).
33. P. H. Holloway, K. Shanker, R. B. Pettit and R. R. Sowell, Oxidation of electrodeposited black chrome selective surfaces. *Thin Solid Films* **72**, 121 (1980).
34. P. M. Driver, An electrochemical approach to the characterization of black chrome selective surfaces. *Sol. Energy Mat.* **4**, 179 (1981).
35. G. B. Smith and A. Ignatiev, Black chromium—

molybdenum a new stable solar absorber. *Sol. Energy Mat.* **4**, 119 (1981).
36. A. Andersson, O. Hunderi and G. Granqvist, Nickel pigmented anodic aluminum oxide for selective absorption of solar energy. *J. appl. Phys.* **51**, 754 (1980).
37. C. Homhual, O. T. Inal, L. E. Murr, A. E. Torma and I. Gündiler, Microstructural and mechanical property evaluation of zinc oxide coated solar collectors. *Sol. Energy Mat.* **4**, 309 (1981).
38. H. Potdar, N. Pavaskar, A. Mitra and A. P. B. Sinha, Solar selective copper black layers by an anodic oxidation process. *Sol. Energy Mat.* **4**, 291 (1981).
39. C. M. Lampert, Selective absorber coated foils for solar collectors. *Plating and Surface Finishing* **67**, 52 (1980).
40. G. L. Harding and B. Window, Graded metal carbide solar selective surfaces coated onto glass tubes by a Magetron sputtering system. *J. Vac. Sci. Technol.* **16**, 2101 (1979).
41. S. Craig and E. L. Harding, Solar selective properties of rough sputtered copper films. *Sol. Energy Mat.* **4**, 245 (1981).
42. J. A. Thornton, A. S. Penfold and J. L. Lamb, *Development of Selective Surfaces*. U.S. DOE Report DE-AC04-78CS35306 (August 1980).
43. E. E. Chain, K. Seshan and B. O. Seraphin, Optical and structural properties of black Mo photothermal converter layers deposited by the pyrolysis of $Mo(CO)_6$. *J. appl. Phys.* **52**, 1356 (1981).
44. J. Mason and T. Brendel, Maxorb—A new selective surface on nickel. *Proc. SPIE* **324**, 139 (1982).
45. J. A. Thornton and J. L. Lamb, *Development of Selective Surfaces*. DOE Report DE-AC04-80AL13116 (December 1981).
46. M. Sikkens, Spectrally selective properties of reactively sputtered NiC and NiN_x films. *Proc. SPIE* **324**, 131 (1982).
47. F. H. Cocks, M. J. Peterson and P. L. Jones, The dependence of the texture of tellurium films on vacuum deposition angle. *Thin Solid Films* **70**, 297 (1980).
48. D. C. Booth, O. Allred and B. O. Seraphin, Stabilized CVD amorphous silicon for high temperature photothermal solar energy conversion. *Sol. Energy Mat.* **2**, 107 (1979).
49. S. B. Gadgil, R. Thangaraj, J. V. Iyer, A. K. Sharma, B. K. Gupta and O. P. Agnihotri, *Sol. Energy Mat.* **5**, 129 (1981).
50. G. B. Smith, A. Ignatiev and G. Zajac, Solar selective black cobalt: preparation, structure and thermal stability. *J. appl. Phys.* **51**, 4186 (1980).
51. W. Kruidhof and M. Van der Leij, Cobalt oxide as a spectrally selective material for use in solar collectors. *Sol. Energy Mat.* **2**, 69 (1979).
52. J. I. Gittleman, E. K. Sichel and Y. Arie, Composite semiconductors: selective absorbers of solar energy. *Sol. Energy Mat.* **1**, 93 (1979).
53. P. Swab, S. V. Krishnaswamy and R. Messier, Characterization of black Ge selective absorbers. *J. Vac. Sci. Technol.* **17**, 1 (1980).
54. G. A. Nyberg, H. G. Graighead and R. A. Buhrman, Roughned, Graded index, cermet photothermal absorbers with very high absorptivities. *Proc. SPIE* **324**, 117 (1982).
55. Y. Noguchi, K. Naka, A. Isao, K. Nakamura, S. Sawada, T. Tani and S. Gonda, Fabrication of ZrCx/Zr and Cr–CrO_x films for practical solar selective absorption systems. *Proc. SPIE* **324**, 124 (1982).
56. E. Erben, A. Muehlratzer, B. Tihanyi and B. Cornils, Development of selective absorber coatings for high temperature application. *Sol. Energy Mat.* **9**, 281 (1983).
57. T. J. McMahon and S. N. Jasperson, PbS–Al selective solar absorbers. *Appl. Optics* **13**, 2750 (1974).
58. H. C. Hottel and T. A. Unger, The properties of a copper oxide—aluminum selective black absorber of solar energy. *Sol. Energy* **3**, 10 (1959).
59. C. N. Watson-Munro and C. M. Horwitz (1975), cited by Meniel [29].
60. H. C. Van deHulst, *Light Scattering by Small Particles*. Dover, New York (1983).
61. I. T. Ritchie, S. K. Sharma, J. Valignat and J. Spitz, Thermal degradation of chromium black solar selective surfaces. *Sol. Energy Mat.* **2**, 167 (1980).
62. C. M. Lampert, *Chemical, Structural and Optical Characterization of a Black Chrome Solar Selective Absorber*. Lawrence Berkeley Laboratory Report LBL-9123 (1979).
63. J. Spitz, T. V. Danh and A. Aubert, Chromium black coatings for photothermal conversion of solar energy, Part 1: preparation and structural characterization. *Sol. Energy Mat.* **1**, 189 (1979).
64. C. M. Lampert and J. Washburn, Metallurgical analysis and high temperature degradation of the black chrome solar selective absorber. *Thin Solid Films* **72**, 75 (1980).
65. P. Driver and P. G. McCormick, Black chrome selective surfaces I, II. *Sol. Energy Mat.* **6**, 159, 381 (1982).
66. J. C. C. Fan and S. A. Spura, Selective black absorbers using RF-sputtered Cr_2O_3/Cr cermet films. *Appl. Phys. Lett.* **30**, 511 (1977).
67. J. H. Lin and R. E. Peterson, Improved black nickel coatings for flat plate solar collectors. *Proc. SPIE* **85**, 62 (1976).
68. H. Tabor, Selective radiation. *Bull. Res. Counc. Isrl* **5A**, 119 (1956).
69. G. Burrafato, G. Giaquinta, N. A. Manciai, A. Pennisi and S. O. Troia, Thin film solar acceptors. In *Heliotechnique and Development*, (Edited by M. Kettani and J. Sossou) Devel. Analysis Assoc., New York (1977).
70. J. C. M. Garnett, Colours in metal glasses, in metallic films. *Phil. Trans. R. Soc., Lond.* **203A**, 385 (1904).
71. J. C. M. Garnett, Colours in metal glasses, in metallic films and in metallic solutions. *Phil. Trans. R. Soc., Lond.* **205A**, 237 (1906).
72. D. A. G. Bruggeman, Berechnung verschiedener physikalischer Konstanten van heterogenen Substanzen. *Annln Phys.* **24**, 636 (1935).
73. C. G. Granqvist, Optical properties of cermet materials. *J. Physics* **42**, C1 (1981).
74. G. W. Milton, Bounds on the complex dielectric constant of a composite material. *Appl. Phys. Lett.* **37**, 300 (1980).
75. D. J. Bergman, Exactly solvable microscopic geometrics and rigorous bounds for the complex dielectric constant of a two component composite material. *Phys. Rev. Lett.* **44**, 1285 (1980).
76. G. A. Niklasson and C. G. Granqvist, Photothermal conversion with cermet films: implications of the bounds on the effective dielectric function. *Sol. Energy Mat.* **5**, 173 (1981).
77. R. E. Peterson and J. Ramsey, Solar absorber study, U.S. Air Force Materials Lab. Wright Patterson AFB, Ohio, AFML-TR-73-80 (1973).

78. S. Lofving, A paint for selective solar absorbers. *Sol. Energy Mat.* **5**, 103 (1981).
79. S. W. Moore, Solar absorber selective paint research. *Sol. Energy Mat.* **12**, 435–449 (1985).
80. R. M. Winegarner, Coating costs and project independence. *Photonics Spectra* **9**, 20 (1975).
81. S. Catalanotti, V. Cuomo, G. Piro, D. Ruggi, V. Silvestrini and G. Troise, The radiative cooling of selective surfaces. *Sol. Energy* **17**, 83 (1975).
82. F. Sakkal, M. Martin and P. Berdahl, Experimental test facility for selective radiative cooling surfaces. *Proc. 4th Natl Passive Solar Conf.* **4**, 483 (1979).
83. T. S. Eriksson, E. M. Lushihu and C. G. Granqvist, Materials for radiative cooling to low temperatures. *Sol. Energy Mat.* **11**, 141 (1984).
84. E. M. Lushihu and C. G. Granqvist, Radiative cooling with selectively infrared emitting gases. *Appl. Optics* **23**, 1835 (1984).
85. G. L. Jorgenson, *Long Term Glazing Performance*. SERI Report TP-31-193 (June 1979).
86. J. Jurison, R. E. Peterson and H. Y. B. Mar, Principles and applications of selective solar coatings. *J. Vac. Sci. Technol.* **12**, 101 (1975).
87. E. M. Pastirik and M. C. Keeling, A low cost, durable antireflective film for solar collectors. *Proc. IEEE 13th Photovoltaic Specialists Conference*, Washington DC, 620 (5–8 June 1978).
88. C. M. Lampert, Optical films for solar energy applications. *Proc. SPIE* **387**, 36 (1983).
89. P. K. Lee and M. K. Debe, Measurement and modeling of the reflectance-reducing properties of graded index microstructured surfaces. *Photo. Sci. Engng* **24**, 211 (1980).
90. M. Rubin and S. Selkowitz, Thermal performance of windows having high solar transmittance. *Proc. Sixth Natl Passive Sol. Conf.* pp. 141–145 (1981).
91. H. Dislich and E. Hussman, Amorphous and crystalline dip coatings obtained from organometallic solutions: procedures, chemical processes and products. *Thin Solid Films* **77**, 129 (1981).
92. C. J. Brinker and M. S. Harringston, Sol-gel derived antireflective coatings for silicon. *Sol. Energy Mat.* **52**, 159 (1981).
93. H. Vora and T. J. Moravec, Structural investigation of thin films of diamond-like carbon. *J. appl. Phys.* **52**, 6151 (1981).
94. M. A. Lind, (ed.), Proc. of the second solar-reflective materials workshop. *Sol. Energy Mat.* **3**, 1 (1980).
95. C. F. Jefferson, H. Myers and F. Russo, Solar reflectors made from silver metallo-organic resinates. *Proc. SPIE* **324**, 74 (1982).
96. R. B. Pettit and E. P. Roth, in *Solar Materials Science* (Edited by L. Murr). Academic Press, New York (1980).
97. B. L. Butler and R. B. Pettit, Optical evaluation techniques for reflecting solar concentrators. *Proc. SPIE* **114**, 43 (1977).
98. A. Goetzberger and V. Wittwer, Fluorescent planar collector-concentrators: a review. *Sol. Cells* **4**, 3 (1981).
99. A. Goetzberger and W. Greubel, Solar energy conversion with fluorescent concentrators. *Appl. Phys.* **14**, 123 (1977).
100. V. Wittwer, W. Stahl and A. Goetzberger, Fluorescent planar concentrator. *Sol. Energy Mat.* **11**, 187 (1984).
101. W. Stahl and V. Wittwer, Highly selective narrowband absorbers in combination with fluorescent concentrators. *Proc. SPIE* **428**, 187 (1983).
102. J. A. Levitt and W. H. Weber, Materials for luminescent greenhouse solar collectors. *Appl. Optics* **16**, 2684 (1977).
103. A. Bennett and L. Olsen, Analysis of multiple cell concentrator-photovoltaic systems. *Proc. IEEE Photov. Spec. Conf.* **13**, 868 (1978).
104. L. De Sandre, D. Y. Sing, H. A. Macleod and M. R. Jacobson, Thin film multilayer filter designs for hybrid solar energy conversion systems. *Proc. SPIE* **562**, 155 (1985).
105. M. A. C. Chendo, D. E. Osborn and R. Swenson, Analysis of spectrally selective liquid absorption filters for hydrid solar energy conversion. *Proc. SPIE* **562**, 160 (1985).
106. J. Jannson, T. Jannson and K. H. Yu, Solar control tunable lippman holowindows. *Proc. SPIE* **562**, 75 (1985).
107. G. Kienel and W. Dachselt, Cold light mirrors. *Ind. Res. Devel.* **22**, 135 (1980).
108. R. Winegarner, Greenhouse selective baffle collector. *Proc. ISES, American Section*, p. 33 (1977).
109. M. R. Brambley and M. Godec, Effectiveness of low emissivity films for reducing energy consumption in greenhouses. *Proc. ASES*, p. 25 (1982).
110. M. Rubin and C. M. Lampert, transparent insulating silica aerogels. *Sol. Energy Mat.* **11**, 1 (1984).
111. J. Fricke, ed. *Aerogels*. Springer, Berlin (1986).
112. J. H. Mazur and C. M. Lampert, High resolution electron microscopy study of silica aerogel transparent insulation. *Proc. SPIE* **502**, 123 (1984).
113. R. Exelby and R. Grintner, Phototropy and photochromism. *Chem. Rev.* **64**, 247 (1964).
114. G. Brown and W. Shaw, Phototropism. *Rev. Pure Appl. Chem.* **11**, 2 (1961).
115. G. H. Dorion and A. F. Wiebe, *Photochromism*. Focal Press, London (1970).
116. G. P. Smith, Photochromic glass: properties and applications. *J. Mat Sci.* **2**, 139 (1967).
117. N. Y. C. Chu, Photochromic performance of spiroindolinonaphthoxazines in plastics. *Proc. SPIE* **562**, 6 (1985).
118. J. H. Day, Chromogenic materials. In *Encyclopedia of Chemical Technology*. Wiley, New York (1977).
119. G. V. Jorgenson and J. C. Lee, Thermochromic materials research for optical switching films. *Proc. SPIE* **562**, 2 (1985).
120. J. C. Lee, G. V. Jorgenson and R. J. Lin, Thermochromic materials research for optical switching. *Proc. SPIE* **692**, 3 (1986).
121. C. M. Lampert, Electrochromic materials and devices for energy efficient windows. *Sol. Energy Mat.* **11**, 1 (1984).
122. W. C. Dautremont-Smith, Transition metal oxide electromic materials and displays: a review. *Displays* **4.3**, 67 (1982).
123. B. W. Faughan and R. S. Crandall, Electrochromic displays based on WO_3. In *Display Devices* (Edited by J. I. Pankove). Springer, Berlin (1980).
124. J. S. E. M. Svensson and C. G. Granqvist, Electrochromic coatings for "Smart windows". *Sol. Energy Mat.* **12**, 391 (1985).
125. J. Nagai, T. Kamimori and Mizuhashi, Transmissive electrochromic device. *Proc. SPIE* **562**, 39 (1985).
126. D. K. Benson and C. E. Tracy, Amorphous tungsten

oxide electrochromic coatings for solar windows. *Proc. SPIE* **562**, 46 (1985).
127. R. B. Goldner, R. L. Chapman, G. Foley, E. L. Goldner, T. Hass, P. Norton, G. Seward and K.-K. Wong. Recent research related to the development of electrochromic windows. *Proc. SPIE* **562**, 32 (1985). development of electrochromic windows. *Proc. SPIE* **562**, 32 (1985).
128. S. F. Cogan, E. J. Anderson, T. D. Plante and R. D. Rauh. Materials and devices in electrochromic window development. *Proc. SPIE* **562**, 23 (1985).
129. C. M. Lampert, T. R. Omstead and P. C. Yu. Chemical and optical properties of electrochromic nickel oxide films. *Sol. Energy Mat.* **14**, 14 (1986).
130. P. C. Yu, G. Nazri and C. M. Lampert. Spectroscopic and electrochemical studies of electrochromic hydrated nickel oxide films. *Proc. SPIE* **653**, 16 (1986).
131. S. Chandrasekhar. *Liquid Crystals*. Cambridge University Press, Cambridge (1977).
132. S. Sherr, *Electronic Displays*. Wiley, New York (1970).
133. J. L. Fergason. Polymer encapsulated nematic liquid crystals for display and light control applications. *SID Digest* **85**, 68 (1985).